Journal of Applied Phycology: https://doi.org/10.1007/s10811-020-02049-9

Acclimation of the microalga *Amphidinium carterae* to different nitrogen sources. Potential application in the treatment of marine aquaculture effluents

A. Molina-Miras[1], L. López-Rosales[1], M.C. Cerón-García[1], A. Sánchez-Mirón[1], A. Olivera-Gálvez[2], F. García-Camacho[1*], E. Molina-Grima[1]

[1]Department of Chemical Engineering, Research Centre CIAIMBITAL, University of Almería, 04120 Almería, Spain

[2]Departamento de Pesca e Aquicultura, Universidade Federal Rural de Pernambuco - UFRPE, Dois irmãos, Recife, Pernambuco, CEP: 52171-900, Brasil.

*Corresponding author: fgarcia@ual.es

Address: Department of Chemical Engineering, University of Almería. Carretera Sacramento s/n. E04120, Almería, Spain.

Telephone number: +34 950015303; e-mail address: fgarcia@ual.es

Journal of Applied Phycology: https://doi.org/10.1007/s10811-020-02049-9

Abstract

There is growing interest in finding microalgae species that efficiently convert dissolved nutrients contained in aquaculture effluents into highly valuable biomass. The different nitrogen forms that are present in aquaculture effluents are particularly concerning. This study demonstrated that the dinoflagellate microalga *A. carterae* can acclimate to both combined and sole nitrogen sources such as nitrate, ammonium and urea over a wide concentration range. As far as is known, it is the first time that a species of the genus *Amphidinium* has been successfully cultured with urea as the sole source of nitrogen. In the presence of 882 µM of nitrate, *A. carterae* tolerated urea concentrations up to 5000 µM. With respect to ammonium-N tolerance, it has been observed that it is lethal at concentrations higher than 441 µM. A robust laboratory experimental design was critical for accurately assessing this acclimation. Alternative N sources did not affect the production of high-value specific polyketide secondary metabolites from *A. carterae*, such as amphidinols, with an average concentration of 0.435 ± 0.038% biomass d.w. An analysis of the symbiotic microbial assemblages developed in a long-term *A. carterae* culture in an open raceway pond, and the fact that it is able to metabolize all three nitrogen sources simultaneously, supports the idea that this microalga has the potential to be successfully cultured with aquaculture effluents.

Keywords: dinoflagellate; *Amphidinium*; urea; ammonium; nitrate; aquaculture

.

1. Introduction

The environmental and social impacts resulting from the aquaculture industry have been comprehensively reviewed (Jegatheesan et al. 2011). In extensive aquaculture systems, the effluents are rich in nutrients, which are highly polluting if released untreated into the sea. Aquaculture wastewater includes particulate organic matter, organics, dissolved metabolites such as ammonia, urea and carbon dioxide, and feed nitrogen and phosphorous that has not been retained by the fish. At much lower proportions, the effluents might also contain other contaminants such as metals, dioxins, organohalogens, and agrochemicals (e.g. pesticides, antifungals, disinfectants or fertilizers). However, one of the main problems associated with partially treated or untreated aquaculture effluent being discharged into natural water bodies is the eutrophication caused by an excess of nitrogen and phosphorous.

Algal blooms are evidence of eutrophication in coastal waters. Dinoflagellates, diatoms, raphidophytes, prymnesiophytes and silicoflagellates are the microalgae groups reported to be presumably responsible (Landsberg 2002). This ability of the microalgae to thrive in eutrophicated waters is probably one of the underlying reasons for their use in studies focused on microalgae-based effluent re-use and/or treatment systems. In this regard, the biofloc systems stands out (BFT; Biofloc Technology) (Crab et al. 2007; Marinho et al. 2017; Wasielesky Jr et al. 2006). However, BFT has still to overcome important challenges since its large-scale application is limited and the effective abatement of the main contaminants is an unresolved issue. Other microalgae have provided interesting results in laboratory-scale cultures of freely-suspended cells (Attasat et al. 2013).

Interestingly, the incidence of algal blooms in marine environments is dominated by dinoflagellates rather than non-dinoflagellate microalgae (Landsberg 2002). This might be explained by the fact that most marine dinoflagellates are able to grow in mixotrophic environments (Burkholder et al. 2008); i.e., they can simultaneously photosynthesize and use organic sources of carbon for growth, and they

are able to take up and store substantial amounts of various N forms (Dagenais-Bellefeuille and Morse 2013). In general, dinoflagellates seem to proliferate more in summer when regenerated, reduced forms of N make up a large proportion of the available N pool (Davidson et al. 2012). Mixotrophic consumption of dissolved organic matter (DOM) by dinoflagellates has also been extensively reviewed (Davidson et al. 2012). The mixotrophic growth rates reported are usually higher than those determined in photoautotrophic cultures. Laboratory studies have confirmed DOM utilization in the form of urea by a few marine dinoflagellate species, finding that urea supported similar growth rates to those using NO_3^- or NH_4^+ as the substrate (Solomon et al. 2010).

Nonetheless, as far as we know, dinoflagellates have never been utilized for the treatment of aquaculture effluents. Only one study reported the satisfactory use of a marine dinoflagellate for municipal wastewater treatment at the laboratory scale (Ho et al. 2013) but not in aquaculture. It is evident that the potential of using aquaculture effluent for the cultivation of marine dinoflagellate microalgae should be explored. Candidate species may be those having a specific biotechnological significance (Gallardo-Rodríguez et al. 2012). In particular, *Amphidinium carterae* is attractive because it produces interesting compounds (Abreu et al. 2019; Molina-Miras et al. 2018a; Molina-Miras et al. 2018b): (i) the polyunsaturated fatty acids EPA (eicosapentaenoic acid) and DHA (docosahexaenoic acid), which have numerous nutraceutical and pharmaceutical applications; (ii) the carotenoid peridinin, which possesses unique photophysical properties and can potentially be used in medicine as a therapeutic agent against various diseases; and (iii) polyketide metabolites, which are potently bioactive. Specific polyketide secondary metabolites from dinoflagellates, such as amphidinolides and amphidinols (APDs) from *A. carterae*, with potent anticancer, antibacterial and antifungal activities are particularly attractive and are priority objective of dinoflagellate based bioprocess. Recent studies have addressed the challenge that arises from recovering the largest amount of the relatively minority metabolites (APDs) while minimising the loss of other valuable by-products (López-Rodríguez et al. 2019).

Moreover, *A. carterae* has been successfully cultured in pilot-scale photobioreactors in photoautotrophic nutritional mode (Molina-Miras et al. 2018a; Molina-Miras et al. 2018b).

Different combinations of cell transporters acting on the nitrogen sources present in aquaculture effluent, each with their own particular kinetics and levels of expression and activity, may operate simultaneously in microalgae, particularly in dinoflagellates (Dagenais-Bellefeuille and Morse 2013). As a result, the large intra- and inter-specific variability of the kinetic parameter values reported in the literature may be partially justified. However, another source of variability might be associated with the experimental design and, particularly, with the culture timescale. Kinetic parameter values in the same dinoflagellate strain can vary from short-term to long-term experiments by more than one order of magnitude (Collos et al. 2007; Harrison 1976). There is a need for better designed laboratory experiments to reduce variability caused by acclimation. The acclimation of some non-dinoflagellate microalgae to a nitrogen source might take at least one cultivation before consistent μ_{max} can be determined for comparative purposes (Podevin et al. 2015). Appropriately evaluating acclimation to new culture conditions is essential for determining a microalga's preference to a specific culture medium, particularly in the case of macronutrients.

Consequently, this work aims to assess and compare the kinetic parameters of the marine dinoflagellate microalga *Amphidinium carterae* on different dissolved inorganic (NO_3^- and NH_4^+) and organic (urea) nitrogen sources. These N forms are usually present in aquaculture effluents at varying concentrations. Experiments were carried out in batch cultures of freely suspended cells. The initial concentrations of urea-N and ammonium-N in the culture medium varied from 0 to 5000 µM, while nitrate-N were between 0 and 1764 µM. The acclimation response of the cells to each combination of assayed N-forms and concentrations was evaluated by repeated subcultivation. The production of APDs was determined in cultures that attained acclimation in the most important kinetic parameters.

The potential application of *A. carterae* in the treatment of marine aquaculture effluents was analyzed based on its ability to (i) remove the nitrogen and phosphorous dissolved in a culture medium and (ii) form an associated bacterial community during long-term culture in a pilot-scale open raceway pond (ORP) (nitrate was used as the nitrogen source).

2. Materials and methods

2.1. The microalga

The marine dinoflagellate microalga *Amphidinium carterae* (strain Dn241 EHU) was used. It was obtained from the Culture Collection of the Plant Biology and Ecology Department of the University of the Basque Country. Inocula were grown in flasks at 21 ± 1 °C placed in a thermostated chamber under a 12:12 h light–dark cycle. Four 58 W fluorescent lamps were used for illumination and the irradiance at the surface of the culture flasks was 60 µE m^{-2} s^{-1}. The f/2 medium, prepared with filter-sterilized (0.22 µm Millipore filter; Millipore Corporation, Billerica, MA, USA) Mediterranean seawater, was used both for inocula maintenance and as the basis for the experiments. The f/2 medium composition was as follows (Guillard, 1975): $NaNO_3$, 882 µM; NaH_2PO_4 H_2O, 36.2 µM; Na_2SiO_3 $9H_2O$, 106 µM; $FeCl_3.6H_2O$, 11.7 µM; Na_2EDTA $2H_2O$, 11.7 µM; $CuSO_4$ $5H_2O$, 0.04 µM; Na_2MoO_4 $2H_2O$, 0.03 µM; $ZnSO_4$ $7H_2O$, 0.08 µM; $CoCl_2$ $6H_2O$, 0.04 µM; $MnCl_2$ $4H_20$, 0.9 µM; Thiamine, 0.3 µM; Biotin, 2.1 nM; B12, 0.37 nM. The f/2 medium has a N:P molar ratio of 24.

2.2. Growth Experiments

The influence of both the nitrogen source and its concentration on the *A. carterae* culture was investigated as described below. Experiments consisted of static batch cultures conducted in vertically arranged T-flasks (ref. 169900 Nunc, EasYFlask 25cm^2 Thermo Fisher Scientific) with a 50 mL working volume, equivalent to a 4.7 cm culture height. The lighting system used was similar to that described by Molina-Miras

et al. (Molina-Miras et al. 2018b) for photoacclimation experiments. In this device the light source was multicolored light emission diodes (LEDs). Parallel LED strips were attached to a flat reflective plastic (PVC) cover and the T-flasks were arranged arranged vertically in front of them. The illumination system provided a mean irradiance of 400 $\mu E \cdot m^{-2} \cdot s^{-1}$ measured on the T-flask surface facing the LEDs. A 12h/12h light/dark (L/D) cycle was set. The culture system was placed in a thermostatic room at 20±1 ºC. The cells to be used in the experiments were pre-photoacclimated to this illumination regime.

Fifteen media were prepared changing both the nitrogen source and its concentration in the basal f/2 medium formulation. Sodium nitrate ($NaNO_3$) and ammonium chloride (NH_4Cl) were tested as inorganic nitrogen sources and urea (CH_4N_2O) as an organic source. The combinations of the nitrogen sources and the concentration levels are detailed in Table 1. Since the basal phosphate concentration in the f/2 medium (36 µM) has been shown to limit growth in *A. carterae* cultures (Molina-Miras et al. 2018a), excess phosphate was added in all the experiments (181µM; five times the original f/2 medium concentration). Thus, the control medium (CTRL) contained 882 µM of nitrate-N and 181 µM of phosphate-P (a N:P molar ratio of 5). The assays, summarized in Table 1, allowed us to assess the effect of (i) each of the three nitrogen sources individually (experiments 1-3; coded as CTRL, URE and AMO, respectively); (ii) increasing urea concentrations (experiments 1 and 3-7) (coded as URE and URE1-4, respectively); (iii) increasing concentrations of NH_4Cl (experiments 1, and 8-11; coded as AMO and AMO1-4, respectively) - both (ii) and (iii) were in the presence of 882 µM of nitrate-N; and (iv) the simultaneous presence of the three nitrogen sources at different concentrations (experiments 12-15; coded as NUE1-4). Most of the concentrations in each of the combinations detailed in the Table 1 significantly exceeded those reported in typical aquaculture effluents as will be discussed below in section 3.8. The cultures were inoculated with cells in linear growth phase. The initial cell concentration in the freshly inoculated T-flasks was around 4.5 ±

1.5×10^4 cell mL^{-1}. Each experiment was conducted in duplicate. To study the cellular acclimation to each of the culture medium compositions assayed, the entire experimental design of Table 1 was repeated three times, i.e. three subcultures were performed in each experiment (this involved 78 batch culture experiments in total). Cells grown in any given formulation (shown in Table 1) in the first subcultivation were transferred to the same freshly prepared medium and subcultured again in a second batch culture; the cells obtained were then finally subcultured in a third subcultivation. For this, a culture fraction was transferred to a fresh growth medium.

The initial pH for all the cultures was fixed at 8 using an acid (0.1 M HCl) or base (0.1 M NaOH). The pH of the culture is particularly relevant for the assays with NH_4Cl (Experiments 2 and 8-15 in Table 1). Ammonium and urea were added aseptically after autoclaving the culture medium to avoid the evaporation of either (Harisson and Berges 2005). At a seawater pH of 8.0 at 20 ºC, only around 10% of the total ammonia is present as the more toxic form, ammonia (NH_3) (Spotte and Adams 1983). Since most of the initial total nitrogen at 8 pH (close to 90%) was present as NH_4^+, nitrogen from NH_4Cl would be referred to NH_4^+-N or ammonium-N indistinctly, even though both ammonia and ammonium were present at the initial fixed pH. The pH was allowed to evolve freely in all the cultures.

2.3. Analytical measurements

Using samples taken throughout the culture, the biomass dry weight was determined as described previously (Molina-Miras et al. 2018b). All the analyses were performed in triplicate. In this way, a biomass concentration calibration curve, expressed as dry weight (C_B^b) versus optical density at 720 nm (OD720), was determined ((C_B^b (g L^{-1}) = $1.038\times OD_{720}$; r^2= 0.938; n= 66). C_B^b was also found to linearly correlate with the average cell biovolume (V_c) of the sample ((C_B^b (g L^{-1}) = $0.173\times C_B^c\times V_c$; r^2= 0.900; n= 66), where C_B^c was the cell number concentration. Both calibration curves confirmed previous predictions (Molina-Miras et al. 2018a). The

maximum photochemical yield of photosystem II (F_V/F_M) was determined using a pulse amplitude modulation (PAM) chlorophyll fluorometer (Mini-PAM-2500; Heinz Walz GmbH, Effeltrich, Germany), as described previously (López-Rosales et al. 2015). The F_V/F_M value, which is the ratio between the maximum variable fluorescence (F_V) and the maximum fluorescence (F_M) of chlorophyll, is universally considered as an indicator of microalgae cell stress.

Concentrations of the three N-sources and phosphorous in the supernatants obtained at the end of each subcultivation were determined as follows. Nitrate nitrogen (Nitrate-N) was measured using the spectrophotometric methods 4500-P and 4500-N for examination of water published by the American Public Health Association (APHA, 1995). Ammonium nitrogen (NH_4^+-N) was measured colorimetrically using Nessler's method (protocol D1426-08 proposed by the American Society for Testing and Materials (ASTM, 2008)). The generated color from samples and ammonium sulfate standards were measured at 410 nm using a spectrophotometer. Total phosphorus (P_T) and nitrogen (N_T) in supernatants were measured according to the protocols 4500-P and 4500-N, respectively, proposed by the APHA (1995), as reported elsewhere (Molina-Miras et al. 2018b). Urea nitrogen (Urea-N) was estimated using the following balance: Urea-N= N_T – (Nitrate-N + NH_4^+-N). Measurements were carried out in duplicate samples and the average value was used.

To evaluate possible stoichiometric limitations resulting from the medium supply and elemental balancing, the biomass elemental composition was determined as described earlier (Molina-Miras et al. 2018b). Only atoms bound in the main macromolecules (C, O, N, H, S, P) were taken into account. NOCHSP analysis was carried out for the biomass harvested at the end of the subcultivations.

2.4. Hemolytic activity and amphidinol quantification

A. carterae (strain Dn241EHU) contains at least two members of the amphidinol family, namely amphidinol A and its 7-sulfate derivative amphidinol B (Abreu et al.

2019). Their titers were firstly expressed in terms of pg saponin per *A. carterae* cell, the so-called equivalent saponin potency (ESP), as described earlier (López-Rosales et al. 2015). The percentage of APDs in the biomass was determined from the following equation based on principles of quantitative nuclear magnetic resonance (NMR) spectroscopy as reported elsewhere (Henderson 2002):

$$APDs, \%\ d.w. = \left(\frac{n_R}{m_b}\right) \times \left(\frac{I_{APDs}}{I_R}\right) \times M_{APDs} \times 100 \quad (1)$$

where, I_R is the NMR signal intensity of the reference compound, I_{APDs} is the NMR signal intensity of the APDs spectra, n_R are the number of mols of reference standard used in the determinations, M_{APDs} is the average molecular weight of amphidinols A and B ($g \cdot mol^{-1}$) and m_b is the mass of dried biomass in the sample (g). The above parameters were determined as detailed earlier (Abreu et al. 2019). The values of I_{APDs} for the dried biomass obtained from several treatments of Table 1 were estimated from a correlation previously developed (Abreu et al. 2019) :

$$I_{APDs} = \frac{ESP - 122.68}{0.0002} \quad (2)$$

This correlation is only valid for this *A. carterae* strain, and eliminates the need to acquire complicated NMR spectra for biomass extracts.

2.5. Flow cytometric measurements

Flow cytometry was used to quantify the following: cell number concentration (C_B^c); the average equivalent cell diameter (D_e); the side scatter (*SS*) related to cell composition and complexity; and the average autofluorescence intensity at specified wavelengths (López-Rosales et al. 2016). Five measurements were performed per sample and an average value was used. Cell volume (V_c) was calculated as $\pi D_e^3/6$. Fluorescence was measured using three photomultiplier tubes: FL1 (525 nm band-pass (BP)), FL2 (575 nm BP) and FL3 (670 nm long-pass). All flow cytometric

measurements used a CellLabQuanta SC flow cytometer (Beckman Coulter Inc., Brea, CA, USA) equipped with an argon-ion excitation laser (blue light, 488 nm). At least 60,000 cells were analysed per sample. The flow rate was kept at a moderate setting (data rate = 600 events s^{-1}) to prevent interference between cells.

The autofluorescence of native pigments and the morphology of microalgal cells are accurate parameters to track the acclimation of cells to new, particular culture environments (Chen et al. 2017). These cell responses are closely related to the content and distribution of pigment in cells. Thus, the cells were illuminated in the flow cytometer with a 488 nm argon laser light and the mean fluorescence intensities were measured in the three different wavelength ranges (photomultiplier detectors FL1, FL2 and FL3) in such a way that each range was characteristic of a group of pigments. The intensity of the fluorescence signals (*FL1,2,3*) are determined by the pigment quantity and profile contained in the cell (Hyka et al. 2013). The fluorescence detected by FL3 and FL1-FL2 can be used as a proxy for monitoring the chlorophyll and carotenoid content, respectively, when excited at 488 nm (Chen et al., 2017). Recently, mathematical relationships between the cell pigment content or the effective cell attenuation cross-section and the *FL1,2,3,* and *SS* measurements have been reported (Chen et al. 2017; López-Rosales et al. 2016). For comparison purposes, *FL1,2,3* intensities were expressed relative to average cell volume (*Vc*).

2.6. Kinetic parameters

The dimensionless cell concentration C_B^c/C_{Bo}^c versus time (t) data were fitted to the following asymmetric logistic equation (Molina-Miras et al. 2018b):

$$\frac{C_B^c(t)}{C_{Bo}^c} = a + \frac{b}{1+\exp\left(-\frac{t-c}{d}\right)} \quad (3)$$

where a, b, c, and d are fit constants. The cell-specific growth rate μ (day^{-1}) was calculated using the best fit curve of Eq. (3); thus:

$$\mu(t) = \frac{1}{C_B^c(t)}\left(\frac{dC_B^c}{dt}\right) \quad (4)$$

The maximum specific growth rate, μ_{max} (day^{-1}), was determined using the curve obtained from the fit in Eq. (4) to the experimental data. The global cell $P_B^c(t)$ and biomass $P_B^b(t)$ productivities, at a given culture time, *t*, were calculated as follows:

$$P_B^c(t) = \frac{C_B^c(t) - C_{Bo}^c}{t} \quad (5)$$

$$P_B^b(t) = \frac{C_B^b(t) - C_{Bo}^b}{t} \quad (6)$$

The maximum values P_{Bmax}^c and P_{Bmax}^b were determined from Eqs. (5) and (6).

Removal efficiencies of dissolved inorganic nitrogen (DIN), Γ_N, and the dissolved inorganic phosphorous (DIP), Γ_P, were calculated as follows:

$$\Gamma_N\ (\%) = (DIN^o - DIN^f)/\ DIN^o \times 100 \quad (7)$$

$$\Gamma_P\ (\%) = (DIP^o - DIP^f)/\ DIP^o \times 100 \quad (8)$$

the superscripts *o* and *f* represent DIN at the beginning and at the end of the culture, respectively. The equation (7) was applied to each nitrogen source and total nitrogen used in every treatment (i.e. Nitrate-N, Urea-N, NH_4^+-N and N_T).

2.7. Determination of the bacterial flora of A. carterae in a long-term ORP culture

The potential use of marine aquaculture effluents for large-scale cultivation of any microalga also requires that selected microalga is able to develop symbiotic microbial assemblages in long-term unialgal cultures because microalgal-bacterial consortiums are inevitable phenomena when using aquaculture effluents (Milhazes-Cunha and Otero 2017). To evaluate this, we used biomass produced in a previous study with an open raceway photobioreactor (ORP) and using nitrate as the N source (Molina-Miras et al. 2018a). The biomass sample was harvested after 260 days of uninterrupted culture. Thus, 10 mL of culture were centrifuged at 2500×g for 5 min at room temperature. The pellet was resuspended in 1 mL of nuclease-free water and re-centrifuged under the same conditions. Total genomic DNA was extracted from the pelleted microalgae using the Soil DNA Isolation Plus Kit (Norgen Biotek Corp.) and

quantified with the Qubit dsDNA HS Assay Kit (Molecular Probes). Metagenomics analyses were performed on a MiSeq equipment of the Illumina massive sequencing platform, based on the reversible terminators method of the DNA polymerization reaction, using fluorescently labeled nucleotide analogues. In the preparation of the library, two pairs of primers designed against V3 and V4 hypervariable regions of 16S rRNA gene were used. Subsequently a series of raw sequence data was generated. Finally, a basic 16S based-characterization of bacterial population was carried out. For the identification and classification of the different taxonomic levels, the DNA sequences were confronted with the GreenGenes database (released by the Greengenes Database Consortium). The algorithm used to classify each sequence is the RDP -Ribosome Database Project-. The accuracy required for each sequence to be classified at a given taxonomic level ranged from the 98.24% to assign a species to 100% for a sequence to be classified at the Kingdom, Phylum or Class level

2.8. Statistical analyses

One-way ANOVA followed by a post-hoc test (Duncan's test) was performed to determine if there were differences between conditions, i.e. effect of the treatments described in Table 1 and subcultivation within a same treatment. ANOVAs were made with the software Statgraphics Centurion XVIII (StatPoint, Herndon, VA, USA). For the majority of the responses above described (V_C, μ_{max}, C^c_{Bmax}, P^c_{Bmax}, P^b_{Bmax}, *Fv/Fm*, *FL1*, *FL2*, *FL3* and *SS*), the assumptions of normal distribution (Shapiroe Wilk's test) and homogeneity of the variance (Bartlett's test) were not violated. In a few cases they were not met, so that the data were log-transformed and validity was assessed. Statistically significant differences in the mean response amongst the treatments or subcultivations were fixed at a 5.0% significance level threshold (p-value<0.05). The method used to discriminate between the means at the 95.0% confidence level was Fisher's least significant difference (LSD) procedure. The non-linear regressions to fit data to the equation (3) were performed with the same software.

3. Results and discussion

3.1. Kinetic parameters in the acclimation process

After carbon, nitrogen is the second most relevant nutrient consumed by microalga. In natural marine habitats, a wide variety of nitrogen compounds with different oxidation states are accessible to and used by microalgae (e.g. nitrate, nitrite, ammonium, urea, amino acids, proteins, etc.). Microalgae have evolved highly efficient pathways for obtaining and consuming nitrogen nutrients from the surrounding environment where they are found in very diluted forms. These pathways are based on enzyme-mediated series-parallel processes that, in general, obey Michaelis-Menten kinetics and control the overall cell growth. The kinetic parameter values derived from the growth response are usually obtained in laboratory batch culture experiments where the species used have previously been maintained for weeks, months or years under unaltered environmental conditions (i.e. the culture medium composition, growth mode, temperature, irradiance, etc.).

Microalgae cultivation studies concerning the use of inocula acclimated to specific conditions that are different from those prevailing in the photobioreactor culture (e.g. under modified culture medium compositions) are abundant in the literature. Consequently, the cells might undergo a process of acclimation on a species-dependent timescale, the impact on the growth dynamics being a function of the magnitude and direction of the shifts performed (e.g. the type of illumination, the nutrient source and the concentration level etc.) (García-Camacho et al. 2012; Voltolina et al. 1998). However, the basic kinetic parameter values are still reported without ensuring acclimated cell responses. As a result, it is common to find different growth curves and kinetic parameters reported for the same species grown under similar conditions in different laboratories.

In this work, the acclimation of *A. carterae* to different nitrogen sources and initial concentrations of nitrogen was studied (see Section 2.2.). *A. carterae* had been

Journal of Applied Phycology: https://doi.org/10.1007/s10811-020-02049-9

previously maintained over a long period (> 1 year) in f/2 medium (with 882 µM NO_3^--N as the sole nitrogen source). The following kinetic parameters, typically reported in microalgae culture studies, were considered: V_C, μ_{max}, $C_{Bmax}^{c,b}$, $P_{Bmax}^{c,b}$, F_V/F_M, *FL1*, *FL2*, *FL3* and *SS*. Accordingly, in a first set of experiments (Subcultures 1), the cells from the original inoculum were cultured in the T-flasks in batch mode with different nitrogen sources and concentrations, as described in Table 1. The cells grown in each culture medium formulation were then subcultured (i.e. a culture fraction was transferred to a fresh growth medium) in the same medium two more times. The evolution of the C_B^c/C_{Bo}^c experimental values over the time course was obtained for each T-flask culture. The kinetic parameter values determined from the growth curves are displayed in Tables 2-4 and 6. To analyze the effect of the factors involved (subcultivation and treatment) on the variability of the kinetic parameters for each experiment in Table 1, an one-way ANOVAs were carried out as explained in section 2.6. The effect of the subcultivation factor are also shown in Tables 2-4 and 6 (values denoted by a different superscript lowercase letter at each mean value differ significantly at $p<0.05$). The subcultivation had a statistically significant effect on several kinetic parameters. This effect was a function of the N source and the concentration. Arrows representing the direction of shift of each kinetic parameter are included in Tables 2, 3 and 4. The results are discussed in the sections below.

3.2. Acclimation to nitrate

As expected, the kinetic parameters for *Amphidinium caterae* grown in the control (CTRL in Table 2) did not present variability ($p<0.05$) between subcultivations; being in line with a pre-acclimated inoculum of the same culture medium composition at a 882 µM NO_3^--N concentration. The F_v/F_m value did not change significantly, with an average value of 0.51±0.02 by the end of the third subcultivation. Although the cells were healthy, this value was almost 20% below that reported for *A. carterae* grown in photobioreactors (Molina-Miras et al. 2018a; Molina-Miras et al. 2018b). *A. carterae*

has already demonstrated excellent tolerance to nitrate, enduring NO_3^--N levels as high as 2646 µM (equivalent to f/2×3) in PBR cultures and f/2×8 in flasks (Dixon and Syrett 1988a; Molina-Miras et al. 2018a; Molina-Miras et al. 2018b). The mechanisms facilitating this tolerance are still unknown although luxury nitrogen uptake under excess nitrogen conditions may be feasible. For example, the dinoflagellate *Protoceratium reticulatum* is able to accumulate significant amounts of intracellular nitrate in culture media with nitrate levels as high as 8820 µM without it affecting the specific growth rate (Gallardo-Rodríguez et al. 2009). *P. reticulatum* actively transported nitrate against the driving force towards the cell's interior (Gallardo-Rodríguez et al. 2009). Consistent with this, several previous studies on various microalgae have demonstrated the versatility of dinoflagellates in acquiring nitrogen nutrients by possessing a wide range of uptake transporters and assimilation enzymes for different forms of nitrogen (Dagenais-Bellefeuille and Morse 2013; Jing et al. 2017; Zhuang et al. 2015). These transporters can continue to operate in a nitrate-repleted medium. Some non-dinoflagellate microalgae can tolerate nitrate concentrations up to 100 mM (Jeanfils et al. 1993).

3.3. Acclimation to ammonium

The results from the first subculture in the AMO experiment were similar to the CTRL. Acclimation was not observed in any of the kinetic parameters (p<0.05) (see Table 2). However, NH_4^+-N-related toxicity became evident from subculture 2. By the end of the third subculture, there were hardly any intact cells (C_{Bmax}^{c}<5000 cell mL^{-1}). The slow cell decay observed through the subcultures seems to indicate that the NH_4^+-N concentration of 882 µM (AMO) may be close to the tolerance level for this *A. carterae* strain. As a result of the NH_4^+-N-related toxicity, the kinetic parameters for subculture 3 were clearly abnormal. Both μ_{max} and $P_{Bmax}^{c,b}$ had negative values due to the disappearance of cells over the culture time (AMO in Table 2). The *Fv/Fm* declined by nearly 70% compared to subculture 1, suggesting that the photosynthetic capacity was

negatively affected by the NH_4^+-N concentration used. The detrimental effect of ammonium-N on microalgal photosynthesis remains a complex matter. Even though several mechanisms have been proposed for explaining the toxic effects of ammonium-N in microalgae, the primary target of ammonium-N damage in the photosynthetic machinery is still to be identified. Recent advances point to ammonium-N directly inducing photodamage to PSII, and affecting PSI, the electron transport chain and the oxygen-evolving complex; this last one being the main site of damage. Accordingly, a feasible working model of ammonium-N competition between N assimilation and PSII damage is able to convincingly interpret cell tolerance to ammonium-N toxicity (Wang et al. 2018).

The significant concomitant increase in V_C and side scatter (*SS*) was indicative of aberrant cell forms (as confirmed by optical microscopy). The extremely high values of *FL1*, *FL2* and *FL3*, compared to the CTRL, revealed a marked increase in cell pigments. This is consistent with the increase in the *Chla* cell quota, based on biovolume, reported for the dinoflagellate *G. sanguineum* grown in ammonium-N rather than a nitrate-N culture (Levasseur et al. 1993). It is unknown whether this *Chla* increase is a response associated with the PSII repair mechanism boosted by ammonium-N toxicity, as one might hypothesise from the Wang model (Wang et al. 2018).

Experiments with increasing NH_4^+-N concentrations (AMO1 to AMO4 in Table 4), maintaining an 882 μM NO_3^--N concentration in the culture medium, were also dominated by pronounced NH_4^+-N toxicity. With NH_4^+-N at 1000 μM (AMO1), the three subcultivations responded in a similar way to subculture 3 of AMO (882 μM, Table 2). None of the kinetic parameters changed significantly between subcultures (p<0.05), thus indicating acclimation from subculture 1. The interactive effect between NO_3^--N and NH_4^+-N could not be properly evaluated due to the severe NH_4^+-N toxicity experienced by the subculture 1 cells. Nevertheless, it has been reported for *A. carterae* that adding a 250 μM non-toxic NH_4^+-N concentration to a culture grown at 880 μM

NO_3^--N brings about rapid and almost complete inhibition of NO_3^+ uptake (Dixon and Syrett 1988b). As a general rule, dinoflagellates prefer to take up NH_4^+-N at subtoxic levels in the presence of various different N sources (Dagenais-Bellefeuille and Morse 2013). At NH_4^+-N concentrations above 1000 µM (AMO2 to AMO4), the severity of NH_4^+-N damage was such that there were no cells left at the end of any of the subcultures (see Table 4).

Ammonium toxicity in marine microalgae has been associated with the effects of both unionized ammonia (NH_3) and ionized ammonium (NH_4^+). However, it is complicated to measure these forms separately so current chemical procedures measure both forms as total ammonia (NH_3 + NH_4^+). Apparently, the NH_3 form is considered the most toxic because it is readily lipid soluble and crosses cell membranes passively. Thus, toxicity at pH values ≥ 9 is almost solely attributed to NH_3 since its concentration increases markedly as pH increases; whereas at pH values ≤ 8, any toxicity effects are more likely associated with NH_4^+ rather than NH_3 (Erickson 1985). As mentioned in the M&M section, the pH of NH_4Cl cultures remained at around 8. Therefore, the main contribution to inhibition is likely attributed to NH_4^+; nevertheless, NH_3 should not be discarded because, despite being present in a much smaller proportion, its toxicity is greater. Indeed, cultures were carried out without agitation and bubbling, conditions that minimize NH_3 desorption to the atmosphere, and favor NH_3 retention in the broth. The observed low tolerance level of *A. carterae* to NH_4^+-N relative to the CTRL (NO_3^--N) is in line with the results reported in the literature for dinoflagellates. As reported recently (Collos and Harrison 2014), this group of microalgae is the least tolerant compared to the other five microalgae classes (Chlorophyceae, Cyanophyceae, Prymnesiophyceae, Diatomophyceae and Raphidophyceae), with an average ammonium concentration threshold of 1200 µM, close to the 882 µM concentration used in AMO (Table 1). However, the few existing studies on *A. carterae* have reported contradictory results. On this matter, tolerance was reported for a different strain (*A. carterae* Hulburt) at 882 µM NH_4^+-N with growth similar to that of the 882 µM NO_3^--N control (Dixon and

Syrett, 1988b). In contrast, the same authors reported a much lower NH_4^+-N concentration threshold, as low as 143 µM (Dixon and Syrett, 1988a). The differences were not justified nor was the prior acclimation to NH_4^+-N mentioned in either study.

Fig. 1A displays C_B^c/C_{Bo}^c versus time for AMO (882 µM NH_4^+-N as the sole nitrogen source) compared to the CTRL (882 µM nitrate as the sole nitrogen source) corresponding to subcultures 3. Growth inhibition in AMO was evident before day 4; afterwards, toxicity gave rise to significant cell decay. This contrasts with the previous subculture 2, where a lag phase of several days was established without affecting cell survival and coming right after a short exponential growth phase (data not shown). Moreover, the growth kinetics of AMO subculture 1 were similar to the CTRL (data not shown). Such progressive AMO acclimation allows us to clearly illustrate the impact that the choice of a single first subculture would have on interpreting acclimatization to AMO. Studies on long-term microalgae acclimation to nitrogen sources are generally scarce, particularly with ammonium and dinoflagellates. Nevertheless, long lag phases in cells acclimated to NH_4^+-N have been previously observed in cultures with non-dinoflagellate microalgae such as *Chlorella vulgaris* (Przytocka-Jusiak et al. 1977). In contrast, short-term transient responses of algal cells to a pulse of ammonium over a few hours are well-documented for microalgae, including dinoflagellates (recently reviewed in (Collos and Harrison 2014)). The few dinoflagellate species studied also showed a lag period for ammonium uptake, as in AMO subculture 2, with high interspecific variability; this was surprisingly not related to the assayed NH_4^+-N concentrations observed in AMO2 to AMO4 (see Table 3). The severe NH_4^+-related toxicity observed above 1000 µM prevented lag phases to form in AMO2 to AMO4 (Fig. 1B).

3.4. Acclimation to urea

The results from the URE treatment (see Table 2 and Fig. 1A) indicate that *A. carterae* could efficiently assimilate urea as the sole N source and achieve growth rates

and photosynthetic capability comparable to the nitrate control (CRTL). To the best of our knowledge, this is the first time that growth supported by urea-N has been reported for species of the *Amphidinium* genus. Acclimation to urea was evident. Kinetic parameters, except for μ_{max}, *Fv/Fm* and *SS*, changed significantly (p<0.05) from the first subcultivation. The shift direction (*T* in Table 2) in the values for a group of parameters ($C_{Bmax}^{c,b}$, $P_{Bmax}^{c,b}$, *FL1*, *FL2* and *FL3*) descended from the first to second subcultivation and acclimation was confirmed in the third subculture while V_C increased and did not achieve an acclimation value. Compared to the control (CTRL), three groups of parameters could be statistically distinguished in subculture 3: (i) those that remained constant (μ_{max} and *SS*); (ii) those that increased (p<0.05) (V_C and *Fv/Fm*); and (iii) those that decreased (p<0.05) ($C_{Bmax}^{c,b}$, $P_{Bmax}^{c,b}$, *FL1*, *FL2* and *FL3*). The diminished values of C_{Bmax}^{c} and P_{Bmax}^{c} relative to the CTRL were mostly compensated for as consequence of larger cells in UREA (V_c was almost 3-times higher); however, this was insufficient to equal the biomass dry weight yield ($i.e.\, C_{Bmax}^{b}$). The scenario is compatible with an N quote in the cells that is higher under urea-replete conditions (URE) than under nitrate-replete condition (CTRL). This hypothesis is supported by recent studies where the impact of high urea bioavailability on C:N stoichiometry and the sensitivity of urea transporter gene expression to urea availability have been documented for dinoflagellates (Jing et al. 2017).

The decrease in *FL1,2* and *3* indicated a lower cell pigment content compared to the CTRL. This is in line with the *Chla* cell quota reduction reported for other dinoflagellates grown in urea rather than nitrate (Abadie et al. 2015; Levasseur et al. 1993). In the past, it was speculated that this urea-induced decrease in *Chla* quotas, shared by other microalgae, may reflect a N-limited status in the cells (Levasseur et al. 1993). Since the CTRL experiment had the same nitrogen concentration but in the form of nitrate, this explanation seems inadequate, as demonstrated by recent studies highlighting the complexity of N metabolism in dinoflagellates (Dagenais-Bellefeuille and Morse 2013). However, as urea provided in the UREA experiment contained 20%

organic carbon, mixotrophic nutrition may have been feasible. This is supported by the fact that *Fv/Fm* was higher in UREA (see Table 2) as reported for other dinoflagellates in terms of Chl*a*-specific fluorescence yield when grown with urea (Levasseur et al. 1993). In general, mixotrophically grown microalgae produce much lower chlorophyll levels compared to those grown under photoautotrophic conditions, whereas carotenoids production is hardly affected at low irradiances (Azaman et al. 2017).

Table 3 collects the results obtained in the experiments with increasing urea-N concentrations in the presence of 882 μM NO_3^--N (URE1 to URE4). Most of the kinetic parameters achieved acclimation values after the second subculture. A few remained constant (V_C, μ_{max}, *Fv/Fm* and SS) in all the subcultures within each treatment. Overall, the kinetic parameter levels for all the urea-N concentration subcultures assayed were closer to those determined in the CTRL (with only nitrate as the N-source) than those in URE (with only urea as the N-source), particularly the FL1-3 values. The growth curves for C_B^c/C_{Bo}^c versus time in Figure 1C evidence the high tolerance to urea shown by *A. carterae*. The highest μ_{max} value (p<0.05) was determined in URE4 at the maximum urea concentration.

The higher *FL1-3* values in URE1-4 compared to URE suggest a simultaneous urea-N and nitrate-N uptake. Evidence of this can be seen in Table 5. It displays the removal efficiencies of urea-N (Γ_{urea}) and nitrate-N ($\Gamma_{NO_3^-}$) on the basis of measurements of their concentration in the supernatants of URE1-4 as described in the Material and Methods section (Table 5 only includes those treatments for which acclimation was attained in the subcultivation 3). Γ_{urea} varied from 7.4 % to 14.6 %, whereas the $\Gamma_{NO_3^-}$ values were significantly higher, ranging from 26.0 % to 37.4 %. It is, thus, shown that *A. carterae* had more affinity for nitrate than for urea. In fact, the nitrate-N uptake was inhibited by urea-N when the second one was four times or more superior to the first one: 5.34 urea-N mg L^{-1} *vs*. 4.44 nitrate-N mg L^{-1} were removed in URE3 and 10.22 urea-N mg L^{-1} *vs*. 3.21 nitrate-N mg L^{-1} in URE4. Therefore, the

ability of *A. carterae* to simultaneously remove nitrate and urea dissolved in a culture medium is demonstrated.

Interactions between concurrent uptakes of different nitrogen sources by dinoflagellates are not yet completely understood. As mentioned above, ammonium is known to inhibit nitrate and urea uptake but scant information concerning the effects of urea on nitrate uptake is available. An exception is a recent study carried out on the dinoflagellate *Prorocentrum minimum* (Matantseva et al. 2016). In that work, the simultaneous uptake of urea-N and nitrate-N was demonstrated for the first time in a dinoflagellate. Nitrate-acclimated *P minimum* prevalently also consumed urea-N over the concurrent NO_3^--N when these nutrients were simultaneously present in the culture medium. Nitrate-N uptake was also inhibited in the presence of urea-N concentrations well above the urea-N to nitrate-N ratio of 1. In our experiments, this ratio ranged from 1.1 (URE1) to 5.9 (URE4). In any case, *P. minimum* also consumed nitrate-N in the presence of urea-N (Matantseva et al. 2016). In fact, adding urea increased the total-N uptake by *P. minimum* compared to using nitrate as the sole nitrogen source (i.e. without urea). It was suggested that the enzyme urease, present in the transcriptome of *P. minimum*, hydrolysed urea to produce two ammonium ions for every urea molecule according to the urease reaction stoichiometry (Matantseva et al. 2016). As such, the ammonium quota in the cells growing in urea may have been theoretically high, resulting in ammonium-mediated inhibition of the nitrate uptake. However, this hypothesis is not supported by our results with ammonium-N because the *A. carterae* tolerance to this N-source clearly seems to be below 882 µM (see below), far from the 5000 µM of urea-N tolerated. A mechanism regulating enzymatic conversion in the cytosol may be involved in the case of urea in ammonium at non-toxic levels.

3.5. Concurrent acclimation to the three N-sources

The effect of concurrent uptakes of the three nitrogen sources on the acclimation response of *A. carterae* was explored through the experiments NUA1-4

described in the Table 1. The nitrogen concentrations used in NUA1-4 in the form of NO_3^--N and urea-N were below those applied in URE1-3 for which deleterious effects were not observed (see results in section 3.4). In addition, the total nitrogen concentration in NUA1-4 did not exceed those of URE1-3. Accordingly, the supply of NH_4^+-N was the main explanation for the effect observed on the kinetics parameters corresponding to NUA1-4 (see Table 6). In this sense, the growth inhibition in NUA1-3 observed in Fig. 1D revealed also NH_4^+-N-related toxicity in this experiments where the NH_4^+-N concentration was equal or higher than 441 μM. The toxicity was such that, at the end of the third subcultivation or there were no cells left (NUA1-2 in Table 5) or the cells continued to disappear (NUA3 in Table 6). In general terms, the effect of NUA1-3 on the kinetic parameters was similar to that discussed above related to the acclimation to ammonium in presence of nitrate (AMO1-4).

Acclimation for the most of kinetic parameters, except for FL1 and FL3, was only observed in NUA4 (NH_4^+-N was 110 μM). This indicates that the tolerance level of *A. carterae* NH_4^+-N is below 441 μM. On the whole, the kinetic parameter values for NUA4 were closer to those determined in URE1-4 (Table 3) where NH_4^+-N was absence. The presence of NH_4^+-N in NUA4, although in a proportion as low as a 5.9% of total nitrogen added, increased slightly the values FL1-3 compared to URE1-3. This was characteristic in the experiments with ammonium (AMO and AMO1) and nitrate (CTRL) as sole nitrogen sources (Fig. 1A and B).

Similarly to the experiments URE1-4, the higher FL1-3 values in NUA4 compared to URE also seemed to suggest N uptake concurrent from the three N-sources present in NUA4. This is supported by the values of the nitrogen removal efficiencies in NUA4 displayed in Table 5. Results confirmed that *A. carterae* is able to simultaneously remove NH_4^+, $NO_3^-$and urea dissolved in a culture medium. The affinity to the N-source was observed in that order, which is consistent with the general response of dinoflagellates at subtoxic $NH4^+$-N concentrations (Dagenais-Bellefeuille and Morse 2013).

3.6. Effect of the nitrogen sources on kinetic parameters in acclimated cultures

Only the subcultivations 3 of the treatments where acclimation was attained (i.e., CTRL, URE, URE1-4 and NUA5) were considered. A one-way ANOVA was performed for each kinetic parameter determined in Tables 2, 3, 4 and 6. The ANOVA analysis decomposed the variance of each kinetic parameter into two components: one between-group component and other within-group component, with 6 and 7 as degrees of freedom, respectively. For μ_{max} (*F-ratio*=3.46; *p*= 0.065) and *Fv/Fm* (*F-ratio*=1.13 ; *p*= 0.433) there is not a statistically significant difference between the mean value of the parameter from one treatment to another at the 5% significance level. The *Fv/Fm* value averaged for all treatments was 0.557±0.053 and the difference between the absolute maximum and minimum weres about the 26% of the average value. A similar percentage difference was found in a long-term (> 170 days) culture of the same strain in a raceway photobioreactor. In respect of μ_{max}, the multiple range tests determined two homogenous groups: one of them composed by URE4 (average μ_{max}=0.56 ± 0.00 day^{-1}) and the other by the remaining treatments (average μ_{max}=0.376 ± 0.053 day^{-1}). No specific reason was found for this difference. Perhaps in part it is related to the low affinity of *A. carterae* for urea as discussed above. Since URE4 contained the same nitrate concentration as CTRL (882 μM), a fairly high concentration of urea (5000 μM) compared to nitrate was needed to achieve this increase in μ_{max}. At this high urea concentration with respect to nitrate it is unknown as *A. carterae* managed nitrogen metabolism during the exponential phase.

For the remaining kinetic parameters there was a statistically significant difference in the mean value of the parameter between treatments: C^b_{Bmax} (*F-ratio*=23.55; *p*=0.000) , C^c_{Bmax} (*F-ratio*=22.99; *p*= 0.000), P^b_{Bmax} (*F-ratio*= 16.62; *p*= 0.001), P^c_{Bmax} (*F-ratio*= 65.72; *p*=0.000), V_C (*F-ratio*= 31.16; *p*=0.000), *FL1* (*F-ratio*= 47.37; *p*=0.000), *FL2* (*F-ratio*= 14.49; *p*=0.001), *FL3* (*F-ratio*=83.51; *p*=0.000) and *SS* (*F-ratio*= 37.16; *p*=0.000). Although several pairs of means for each kinetic parameter

showed statistically significant differences, not all of them were relevant. Particular attention is drawn to the differences between the treatments URE (urea as the sole nitrogen source) and NUA (concurrent presence of the three N-sources, with subtoxic NH4+-N concentrations). Regarding C_{Bmax}^{b} (g L^{-1}), the averaged value was 0.089 ±0.004 g L^{-1} with a percentage difference between maximum (NUA4) and minimum (URE) around 56% relative to the average value. As the nitrogen and phosphorous contained in the culture medium were not exhausted completely (see Table 5), the maximum biomass capacity of the different treatments based on the elemental composition of *A. carterae* was not achieved. Therefore, the variation in C_{Bmax}^{b} may be also attributed to the different affinity by the N-source because it determines differences in the growth rates of the linear phase as discussed below. Likewise, maximum values of C_{Bmax}^{c}, $P_{Bmax}^{b,c}$ and *FL1-3* were observed for NUA4, while the minimum values were provided by URE. An opposite trend was observed in the cell volume (V_c). The response of V_c in microalgae seems to generally be linked to their nutrient storage capacity (Stolte et al. 1994). As it is also dependent on species and nitrogen source, specific studies should be conducted to address this issue.

3.7. Nutrients removal efficiency and N-balance

Results from Table 5 shown that *A. carterae* was able to remove different dissolved inorganic and organic nitrogen sources and phosphorous. Since the culture experiments were first conceived to study acclimatization, their duration was limited. As result, total nitrogen and phosphorous removal efficiencies (Γ_{N_T} and Γ_{P_T} were far from 100%, indicating nutrients were not exhausted at the end of the culture. This is related with the appearance of a linear growth phase in the cultures as can be seen in Fig 1. A linear growth phase in a batch culture is established when CO_2 and/or light energy consumptions balanced the CO_2 and photons transfer (Contreras et al. 1998). The low light path of the T-Flak (less than 40 mm), a controlled illumination and a relatively low maximum cell concentration in the cultures assured a sufficiency of light during the

culture. On contrast, CO_2 limitation was apparently an issue during most of the culture period because cultures were static and not bubbled with air. Thus, atmospheric CO2 diffusion through culture free surface was the only way for supplying CO_2 to cells. As a consequence, the pH increased over culture time due to the photosynthetic activity of cells confirming the CO_2 limitation. It is reasonable to infer that the Γ_{N_T} and Γ_{P_T} values in Table 5 might be feasibly improved in agitated photobioreactor cultures of *A. carterae* (Molina-Miras et al. 2018a; Molina-Miras et al. 2018b), since they are operated at a constant pH (usually < 8.5) controlled by automatic injection of carbon dioxide, as needed. As a result, there was no carbon limitation; linear phases are thus caused by light limitation and stationary phases by complete exhaustion of growth limiting macronutrients (nitrate and/or phosphate).

Regarding N-balance, the biomass amount harvested in each treatment listed in Table 5 along with its elemental composition allowed us to determine the quantities of the total nitrogen and phosphorous actually fixed in the biomass. These values differed from those contained in the culture medium of each treatment (see Table 1) by less than 4% for phosphorous and a maximum of 20 % for nitrogen in URE4. This lost nitrogen in the N-balance implies the likely existence of another small sink of nutrients incorporating N and P, the main candidate being biofouling layer of *A. carterae* developed on the surface of the T-flasks. This is in line with similar observations previously reported in PBR cultures of *A. carterae* (Molina-Miras et al. 2018a).

Except for CTRL and URE, nitrogen were apparently in excess, as demonstrated by the P-molar formulas in Table 5, since cell N:P molar ratios were higher than the N:P molar ratios in the culture media (see Table 1). This is consistent with the data of nutrient removal efficiency in Table 5, as all values of Γ_{P_T} were higher than the corresponding Γ_{N_T} ones, particularly in URE1-4 and NUA4.

Since the elemental composition of the biomass varied slightly among the treatments, although not systematically, a weighted average elemental composition of 47.9±0.5 (C %), 32.6±0.4 (O %), 7.2±0.1 (H %), 8.0±0.1 (N %), 0.7±0.1 (S %), 3.3±0.1

(P %) was calculated (n=14) for the whole biomass obtained. The corresponding average P-molar formula derived from the above average biomass elemental composition was $C_{37.0\pm0.5}O_{18.9\pm0.2}H_{66.7\pm0.7}N_{5.3\pm0.1}S_{0.2\pm0.1}P_1$, with the molar ratios C:P=37.0, C:N= 7.0 and N:P=5.3. This average P-molar formula is similar to that recently reported for the same strain of *A. carterae* (Molina-Miras et al. 2018a). The low variability observed in the P-molar formula due to effect of the treatments (Table 5) is expected in the context of the changeability of the macronutrient (C:N:P) stoichiometry associated with both phylogenetic differences and the growth conditions as discussed in elsewhere (Molina-Miras et al. 2018a).

3.8. Potential use of marine aquaculture effluents to culture A. carterae.

There is great interest in finding microalgae species that efficiently convert the nitrogen, phosphorous and other dissolved nutrients contained in aquaculture effluents into valuable biomass. However, any species selected must be able to tolerate, and simultaneously reduce, the high ammonium, urea and nitrate concentrations in the effluents. Concentrations of the main nutrients in aquaculture systems reported in different studies are provided in Table 7. Although the presence of urea was only documented in two of the studies, this did not preclude its presence into the rest of effluents. Apparently, several microalgae species could be used with a same effluent (Table 7). However, the characteristics of these effluents may be species-specific and microalgae of particular interest should be tested as mentioned in recent revision works (Milhazes-Cunha and Otero 2017). Regarding the microalga *A. carterae*, the combinations collected in Table 1, whose nutrient concentration levels allowed growth after three subcultivations, have been distributed through the cases referred to in Table 7 in function of whether nutrient concentration levels in a particular effluent are equal or inferior to those of a particular treatment of Table 1. The assignments revealed that in an important percentage of the cases the use of aquaculture effluents for *A. carterae* cultivation as a substitute or a basis to prepare culture media may be feasible.

Although several interesting non-dinoflagellate species (Milhazes-Cunha and Otero 2017) seem to fulfill the requirements above mentioned, none produce high added-value molecules such as those used in pharmacological applications. Dinoflagellates, such as the *Amphidinium* species, which produce bioactive polyketides such as APDs, may be serious candidates (Molina-Miras et al. 2018a; Molina-Miras et al. 2018b). This is supported by the APDs measurements performed in the biomass harvested from the treatments included in Table 7. Thus, APDs were produced in the cultures of the all treatments with a similar average content in the biomass (0.435±0.038 % d.w). This absence of significant differences between treatments was expected since APDs are secondary metabolites that mainly accumulate in stationary phases because their synthesis is strongly stimulated when nitrogen and/or phosphorus are exhausted in the culture medium (Molina-Miras et al. 2018b).

The experimental results presented here show that *A. carterae* can acclimate to varied, combined or sole nitrogen sources over a wide range of concentrations. It is more than likely that this ability may have been exploited by a species in this genus (*Amphidinium eilatiensis* n. sp) to bloom in mariculture ponds, where it survived adapting well to the highly eutrophic environment and can cyclically tolerate (daily and annual) fairly wide ranges of abiotic factors (Lee et al. 2003). These observations were supported by laboratory experiments where *A. eilatiensis* endured the following ranges: temperature (20-32 ºC), salinity (20-40‰), pH (6.5-9), and nutrients (NO_3^- 100-10000 µM; NH_4^+ 900-2800 µM; phosphorous 50-500 µM). *A. eilatiensis* outgrew faster-growing diatom species such as *Navicula*, *Nitzschia*, and *Amphora* (Lee et al. 2003). These characteristics are probably shared by the *Amphidinium* genus strains, including *A. carterae*, explaining their abundance in seas and oceans and their cosmopolitan character, as cited in the literature (Lauritano et al. 2017), making them capable of conquering not only the majority of seas and oceans, but also estuaries and eutrophic coastal areas. The reasons supporting this are varied; for example, substantial experimental evidence shows that dinoflagellates can also uptake particulate and

dissolved organic matter (POM and DOM, respectively) as nutrient sources (Burkholder et al. 2008). Given that effluents from aquaculture ponds contain high levels of POM (from sludges) and DOM (e.g. backwash supernatants), *A. carterae* may contribute to valorizing aquaculture backwash wastewaters; this is because one might expect a growth stimulating effect via mixotrophic or heterotrophic nutritional modes from this microalga. Therefore, if the level of ammonium or ammonia was demonstrated to be inhibitory, photobioreactor performance may be enhanced by pre-treatment of marine aquaculture effluent, either by diluting it with seawater, mixing it with other nutrients (e.g. industrial fertilizers) or treating it with industrial adsorbents to reduce the ammonium concentration.

Open raceway ponds (ORP) are the preferred microalgae photobioreactors for treating aquaculture wastewaters because they need less aeration than the costly mechanical aeration present in conventional activated sludge systems (Li et al. 2019; Sfez et al. 2015). Long-term robust culture of *A. carterae* in ORPs is feasible (Molina-Miras et al. 2018a). The harvested biomass would need further valorization to be turned into a marketable co-product. High value valorization pathways have been recently reported for *A. carterae* biomass grown in photobioreactors (López-Rodríguez et al. 2019; Molina-Miras et al. 2018b), particularly the apocarotenoid peridinin, the polyunsaturated fatty acids EPA and DHA, and polyketide secondary metabolites that exhibit potent anticancer, antifungal and hemolytic activities.

A carterae seems to be a potential microalga for consideration in the Integrated Multi-trophic Aquaculture (IMTA) methodology, a promising alternative strategy for the log-term sustainability and profitability of the aquaculture industry (Li et al. 2019; Milhazes-Cunha and Otero 2017). An *A. carterae* culture facility could occupy one of the biological compartments of a marine IMTA, connected to others by water streams carrying nutrients. However, it is expected that long-term unialgal cultures using aquaculture effluents as the culture medium lead to microalgal-bacterial consortia (Milhazes-Cunha and Otero 2017). In fact, a photoautotrophic long-term

culture of *A. carterae* in an ORP with a culture medium based on the f/2 formulation (nitrate as the N source), as reported elsewhere (Molina-Miras et al. 2018a), ended up being unialgal but not completely axenic. To document (for the first time) the bacterial flora of *A. carterae* in an ORP culture, a sample of broth was withdrawn from the ORP after 260 days of uninterrupted culture, and the bacterial community was examined using a combination of mass-amplification of the short DNA sequences encoding 16S rRNA and high-throughput sequencing, as described in the Materials and Methods section. A total of 19 Phylum-level Taxonomic Categories were identified. The eight most abundant phyla (according to the percentage of total bacterial sequences) were the following: *Proteobacteria* (86.93%), *Bacteroidetes* (10.03 %), *Firmicutes* (1.74%), *Spirochaetes* (0.2%), *Verrucomicrobia* (0.2%), *Actinobacteria* (0.1%), *Planctomycetes* (0.07%) and unclassified phyla (0.63%). The predominant phylum was *Proteobacteria* as anticipated for other dinoflagellates (Zhang et al. 2015b). Figure 2 shows the most prevalent taxonomic categories. The species richness and the diversity of the bacterial community existing within the *A. carterae* sample was in good agreement with recent results reported for dinoflagellates of the genus *Alexandrium*, in which the symbiotic bacterial biodiversity depends on the species (Zhang et al. 2015a). This is consistent with the cell surface characteristics of *A. carterae*. It has small, rounded structures of less than 100 nm that provide an extensive surface area covered by glycocalyx, an adhesive cell-surface coat to which a perfect habitat for bacterial adherents has been attributed (Liu and Place 2017). These observations also support the idea that *A. carterae* has the potential of being successfully cultured with aquaculture effluents since it may develop symbiotic microbial assemblages. In addition, dinoflagellates can phagocytize bacteria and a wide range of eukaryotic prey (Burkholder et al. 2008).

It will be valuable to conduct an interaction study of symbiotic bacteria with the host dinoflagellate in the near future. This could eventually lead to the identification of selective mechanisms operating in ORPs integrated in IMTA systems, which favor specific types of bacterial populations. Obviously, the sources, concentrations and

relative amounts of nitrogen, phosphorous and organic carbon will vary from natural and artificial laboratory environments, and thus may also contribute to the *in vitro* development of bacterial communities dominated by specific taxa.

Future work will be addressed at studying the influence of environmental conditions and wastewater composition on *A. carterae* stability and population density, as well as the microbial community structure, which in turn may modify the wastewater treatment capability and synthesis of interesting metabolites.

4. CONCLUSIONS

A. carterae can acclimate to varied, combined or sole nitrogen sources over a wide range of concentrations. On the basis of nitrogen removal efficiency, the affinity of *A. carterae* to the N-sources was established in the following order: ammonium, nitrate and urea. Our results highlighted the need for better designed laboratory experiments in order to reduce the variability found in the literature due to acclimation. *A. carterae* is able to develop symbiotic microbial assemblages in long-term robust cultures in pilot-scale open raceway ponds (ORP). Since ORPs are the preferred microalgae photobioreactors for treating aquaculture wastewaters, *A. carterae* has the potential to be successfully cultured with aquaculture effluents containing different nitrogen sources, up to 441 µM of ammonia, and to produce biomass that is rich in high added-value metabolites such as amphidinols.

Acknowledgements

This research was funded by the Spanish Ministry of Economy and Competitiveness (CTQ2014-55888-C3-02) and the European Regional Development Fund Program. We are very grateful to the Brazilian National Council for Scientific and Technological Development (CNPq) for the aid granted to Professor Alfredo Olivera-Gálvez (PDE 203104/2017-0). The microalgae *Amphidinium carterae* Dn241 EHU was

kindly donated by Dr. S. Seoane (Culture Collection of the Plant Biology and Ecology Department of the University of the Basque Country).

References

Abadie E, Kaci L, Berteaux T, Hess P, Sechet V, Masseret E, Rolland J, Laabir M (2015) Effect of nitrate, ammonium and urea on growth and pinnatoxin G production of *Vulcanodinium rugosum*. Mar Drugs 13:5642-5656

Abreu AC, Molina-Miras A, Aguilera-Sáez LM, López-Rosales L, Cerón-García MadC, Sánchez-Mirón A, Olmo-García L, Carrasco-Pancorbo A, García-Camacho F, Molina-Grima E (2019) Production of Amphidinols and Other Bioproducts of Interest by the Marine Microalga Amphidinium carterae Unraveled by Nuclear Magnetic Resonance Metabolomics Approach Coupled to Multivariate Data Analysis. J Agric Food Chem 67:9667−9682 doi:10.1021/acs.jafc.9b02821

Andreotti V, Chindris A, Brundu G, Vallainc D, Francavilla M, García J (2017) Bioremediation of aquaculture wastewater from *Mugil cephalus* (Linnaeus, 1758) with different microalgae species. Chem Ecol 33:750-761

Andreotti V, Solimeno A, Chindris A, Marazzi F, García J (2019) Growth of *Tetraselmis suecica* and *Dunaliella tertiolecta* in Aquaculture Wastewater: Numerical Simulation with the BIO_ALGAE Model. Water, Air, Soil Pollut 230:60

Attasat S, Wanichpongpan P, Ruenglertpanyakul W (2013) Cultivation of microalgae (*Oscillatoria okeni* and *Chlorella vulgaris*) using tilapia-pond effluent and a comparison of their biomass removal efficiency. Water Sci Technol 67:271-277

Azaman SNA, Nagao N, Yusoff FM, Tan SW, Yeap SK (2017) A comparison of the morphological and biochemical characteristics of *Chlorella sorokiniana* and *Chlorella zofingiensis* cultured under photoautotrophic and mixotrophic conditions. PeerJ 5:e3473

Borges M-T, Silva P, Moreira L, Soares R (2005) Integration of consumer-targeted microalgal production with marine fish effluent biofiltration–a strategy for mariculture sustainability. J Appl Phycol 17:187-197

Burkholder JM, Glibert PM, Skelton HM (2008) Mixotrophy, a major mode of nutrition for harmful algal species in eutrophic waters. Harmful Algae 8:77-93

Chen J-H, Kato Y, Matsuda M, Chen C-Y, Nagarajan D, Hasunuma T, Kondo A, Dong C-D, Lee D-J, Chang J-S (2019) A novel process for the mixotrophic production of lutein with *Chlorella sorokiniana* MB-1-M12 using aquaculture wastewater. Bioresour Technol 290:121786

Chen J, Wei D, Pohnert G (2017) Rapid estimation of astaxanthin and the carotenoid-to-chlorophyll ratio in the green microalga *Chromochloris zofingiensis* using flow cytometry. Mar Drugs 15:231-253

Collos Y, Harrison PJ (2014) Acclimation and toxicity of high ammonium concentrations to unicellular algae. Mar Pollut Bull 80:8-23

Collos Y, Vaquer A, Laabir M, Abadie E, Laugier T, Pastoureaud A, Souchu P (2007) Contribution of several nitrogen sources to growth of *Alexandrium catenella* during blooms in Thau lagoon, southern France. Harmful Algae 6:781-789

Contreras A, García F, Molina E, Merchuk JC (1998) Interaction between CO 2-mass transfer, light availability, and hydrodynamic stress in the growth of Phaeodactylum tricornutum in a concentric tube airlift photobioreactor. Biotechnol Bioeng 60:317-325

Crab R, Avnimelech Y, Defoirdt T, Bossier P, Verstraete W (2007) Nitrogen removal techniques in aquaculture for a sustainable production. Aquaculture 270:1-14

Dagenais-Bellefeuille S, Morse D (2013) Putting the N in dinoflagellates. Frontiers in Microbiology 4:369 doi:10.3389/fmicb.2013.00369

Davidson K, Gowen RJ, Tett P, Bresnan E, Harrison PJ, McKinney A, Milligan S, Mills DK, Silke J, Crooks A-M (2012) Harmful algal blooms: how strong is the evidence that nutrient ratios and forms influence their occurrence? Estuar Coast Shelf Sci 115:399-413

Deviller G, Aliaume C, Nava MAF, Casellas C, Blancheton JP (2004) High-rate algal pond treatment for water reuse in an integrated marine fish recirculating system: effect on water quality and sea bass growth. Aquaculture 235:331-344

Dixon G, Syrett P (1988a) The growth of dinoflagellates in laboratory cultures. New Phytol 109:297-302 doi:10.1111/j.1469-8137.1988.tb04198.x

Dixon GK, Syrett PJ (1988b) Interactions between the uptake and assimilation of inorganic nitrogen and carbon in *Amphidinium* spp.(Dinophyceae). J Exp Bot 39:1299-1311

Erickson RJ (1985) An evaluation of mathematical models for the effects of pH and temperature on ammonia toxicity to aquatic organisms. Water Res 19:1047-1058

Gallardo-Rodríguez J, Sánchez-Mirón A, García-Camacho F, López-Rosales L, Chisti Y, Molina-Grima E (2012) Bioactives from microalgal dinoflagellates. Biotechnol Adv 30:1673-1684 doi:10.1016/j.biotechadv.2012.07.005

Gallardo-Rodríguez JJ, Sánchez-Mirón A, Cerón-García MdC, Belarbi EH, García-Camacho F, Chisti Y, Molina-Grima E (2009) Macronutrients requirements of the dinoflagellate *Protoceratium reticulatum*. Harmful Algae 8:239-246 doi:http://dx.doi.org/10.1016/j.hal.2008.06.002

Gao F, Li C, Yang Z-H, Zeng G-M, Feng L-J, Liu J-z, Liu M, Cai H-w (2016) Continuous microalgae cultivation in aquaculture wastewater by a membrane photobioreactor for biomass production and nutrients removal. Ecol Eng 92:55-61

García-Camacho F, Sánchez-Miron A, Molina-Grima E, Camacho-Rubio F, Merchuck JC (2012) A mechanistic model of photosynthesis in microalgae including photoacclimation dynamics. J Theor Biol 304:1-15 doi:10.1016/j.jtbi.2012.03.021

Guo Z, Liu Y, Guo H, Yan S, Mu J (2013) Microalgae cultivation using an aquaculture wastewater as growth medium for biomass and biofuel production. Journal of Environmental Sciences 25:S85-S88

Halfhide T, Åkerstrøm A, Lekang OI, Gislerød HR, Ergas SJ (2014) Production of algal biomass, chlorophyll, starch and lipids using aquaculture wastewater under axenic and non-axenic conditions. Algal Res 6:152-159

Harisson PT, Berges JA (2005) Marine culture media. In: Andersen R (ed) Algal culturing techniques. Elsevier Academic Press, Burlington, pp 21–34

Harrison WG (1976) Nitrate metabolism of the red tide dinoflagellate *Gonyaulax polyedra* Stein. J Exp Mar Biol Ecol 21:199-209

Henderson TJ (2002) Quantitative NMR spectroscopy using coaxial inserts containing a reference standard: purity determinations for military nerve agents. Anal Chem 74:191-198

Ho K-C, Xu SJ-L, Wu K-C, Lee FW-F (2013) Effective growth of dinoflagellate *Prorocentrum minimum* by cultivating the cells using municipal wastewater as nutrient source. Water Sci Technol 68:1100-1106

Hussenot J, Lefebvre S, Brossard N (1998) Open-air treatment of wastewater from land-based marine fish farms in extensive and intensive systems: current technology and future perspectives. Aquat Living Resour 11:297-304

Hyka P, Lickova S, Přibyl P, Melzoch K, Kovar K (2013) Flow cytometry for the development of biotechnological processes with microalgae. Biotechnol Adv 31:2-16

Jeanfils J, Canisius M, Burlion N (1993) Effect of high nitrate concentrations on growth and nitrate uptake by free-living and immobilized *Chlorella vulgaris* cells. J Appl Phycol 5:369-374

Jegatheesan V, Shu L, Visvanathan C (2011) Aquaculture effluent: impacts and remedies for protecting the environment and human health. In: Nriagu JO (ed) Encyclopedia of environmental health. Elsevier, Amsterdam, pp 123-135

Jing X, Lin S, Zhang H, Koerting C, Yu Z (2017) Utilization of urea and expression profiles of related genes in the dinoflagellate *Prorocentrum donghaiense*. PLoS One 12:e0187837

Khatoon H, Haris H, Rahman NA, Zakaria MN, Begum H, Mian S (2018) Growth, Proximate Composition and Pigment Production of *Tetraselmis chuii* Cultured with Aquaculture Wastewater. J Ocean Univ China 17:641-646

Landsberg JH (2002) The effects of harmful algal blooms on aquatic organisms. Rev Fish Sci 10:113-390

Lauritano C, De Luca D, Ferrarini A, Avanzato C, Minio A, Esposito F, Ianora A (2017) De novo transcriptome of the cosmopolitan dinoflagellate *Amphidinium carterae* to identify enzymes with biotechnological potential. Sci Rep 7:11701

Lee JJ, Shpigel M, Freeman S, Zmora O, Mcleod S, Bowen S, Pearson M, Szostek A (2003) Physiological ecology and possible control strategy of a toxic marine dinoflagellate, *Amphidinium* sp., from the benthos of a mariculture pond. Aquaculture 217:351-371

Levasseur M, Thompson PA, Harrison PJ (1993) Physiological acclimation of marine phytoplankton to different nitrogen sources 1. J Phycol 29:587-595

Li M, Callier MD, Blancheton J-P, Galès A, Nahon S, Triplet S, Geoffroy T, Menniti C, Fouilland E, Roque d'orbcastel E (2019) Bioremediation of fishpond effluent and production of microalgae for an oyster farm in an innovative recirculating integrated multi-trophic aquaculture system. Aquaculture 504:314-325

Liu C-L, Place AR (2017) Use of Antibiotics for Maintenance of Axenic Cultures of *Amphidinium carterae* for the Analysis of Translation. Mar Drugs 15:242

Liu M, Huang X, Zhang R, Li C, Gu B (2018) Uptake of urea nitrogen by *Oocystis borgei* in prawn (*Litopenaeus vannamei*) aquaculture ponds. Bull Environ Contam Toxicol 101:586-591

López-Rodríguez M, Cerón-García M, López-Rosales L, González-López C, Molina-Miras A, Ramírez-González A, Sánchez-Mirón A, García-Camacho F, Molina-Grima E (2019) Assessment of multi-step processes for an integral use of the biomass of the marine microalga *Amphidinium carterae*. Bioresour Technol

López-Rosales L, García-Camacho F, Sánchez-Mirón A, Beato EM, Chisti Y, Grima EM (2016) Pilot-scale bubble column photobioreactor culture of a marine dinoflagellate microalga illuminated with light emission diodes. Bioresour Technol 216:845-855 doi:10.1016/j.biortech.2016.06.027

López-Rosales L, García-Camacho F, Sánchez-Mirón A, Contreras-Gómez A, Molina-Grima E (2015) An optimisation approach for culturing shear-sensitive dinoflagellate microalgae in bench-scale bubble column photobioreactors. Bioresour Technol 197:375-382 doi:10.1016/j.biortech.2015.08.087

Marinho YF, Brito LO, Silva Campos CVFd, Severi W, Andrade HA, Galvez AO (2017) Effect of the addition of *Chaetoceros calcitrans*, *Navicula* sp. and *Phaeodactylum tricornutum* (diatoms) on phytoplankton composition and growth of *Litopenaeus vannamei* (Boone) postlarvae reared in a biofloc system. Aquacult Res 48:4155-4164

Matantseva O, Skarlato S, Vogts A, Pozdnyakov I, Liskow I, Schubert H, Voss M (2016) Superposition of individual activities: urea-mediated suppression of nitrate uptake in the dinoflagellate *Prorocentrum minimum* revealed at the population and single-cell levels. Frontiers in microbiology 7:1310

Milhazes-Cunha H, Otero A (2017) Valorisation of aquaculture effluents with microalgae: The Integrated Multi-Trophic Aquaculture concept. Algal Res 24:416-424

Molina-Miras A, López-Rosales L, Sánchez-Mirón A, Cerón-García MC, Seoane-Parra S, García-Camacho F, Molina-Grima E (2018a) Long-term culture of the marine dinoflagellate microalga *Amphidinium carterae* in an indoor LED-lighted raceway photobioreactor: Production of carotenoids and fatty acids. Bioresour Technol 265:257-267 doi:https://doi.org/10.1016/j.biortech.2018.05.104

Molina-Miras A, Morales-Amador A, de Vera C, López-Rosales L, Sánchez-Mirón A, Souto M, Fernández J, Norte M, García-Camacho F, Molina-Grima E (2018b) A

pilot-scale bioprocess to produce amphidinols from the marine microalga *Amphidinium carterae*: Isolation of a novel analogue. Algal Res 31:87-98

Nasir NM, Bakar NSA, Lananan F, Hamid SHA, Lam SS, Jusoh A (2015) Treatment of African catfish, *Clarias gariepinus* wastewater utilizing phytoremediation of microalgae, *Chlorella sp*. with *Aspergillus niger* bio-harvesting. Bioresour Technol 190:492-498

Pagand P, Blancheton JP, Lemoalle J, Casellas C (2000) The use of high rate algal ponds for the treatment of marine effluent from a recirculating fish rearing system. Aquacult Res 31:729-736

Podevin M, De Francisci D, Holdt SL, Angelidaki I (2015) Effect of nitrogen source and acclimatization on specific growth rates of microalgae determined by a high-throughput in vivo microplate autofluorescence method. J Appl Phycol 27:1415-1423

Przytocka-Jusiak M, Mlynarczyk A, Kulesza M, Mycielski R (1977) Properties of *Chlorella vulgaris* strain adapted to high concentration of ammonium nitrogen. Acta Microbiol Pol 26:185-197

Riaño B, Molinuevo B, García-González M (2011) Treatment of fish processing wastewater with microalgae-containing microbiota. Bioresour Technol 102:10829-10833

Schulz C, Gelbrecht J, Rennert B (2003) Treatment of rainbow trout farm effluents in constructed wetland with emergent plants and subsurface horizontal water flow. Aquaculture 217:207-221

Sfez S, Van Den Hende S, Taelman SE, De Meester S, Dewulf J (2015) Environmental sustainability assessment of a microalgae raceway pond treating aquaculture wastewater: From up-scaling to system integration. Bioresour Technol 190:321-331

Solomon CM, Collier JL, Berg GM, Glibert PM (2010) Role of urea in microbial metabolism in aquatic systems: a biochemical and molecular review. Aquat Microb Ecol 59:67-88

Spotte S, Adams G (1983) Estimation of the allowable upper limit of ammonia in saline waters. Mar Ecol Prog Ser 10:207-210

Srimongkol P, Tongchul N, Phunpruch S, Karnchanatat A (2019) Ability of marine cyanobacterium *Synechococcus* sp. VDW to remove ammonium from brackish aquaculture wastewater. Agric Water Manage 212:155-161

Stolte W, McCollin T, Noordeloos AA, Riegman R (1994) Effect of nitrogen source on the size distribution within marine phytoplankton populations. J Exp Mar Biol Ecol 184:83-97

Voltolina D, Nieves M, Navarro G, Oliva T, Peraza D (1998) The importance of acclimation for the evaluation of alternative media for microalgae growth. Aquacult Eng 19:7-15

Wang J, Zhou W, Chen H, Zhan J, He C, Wang Q (2018) Ammonium Nitrogen Tolerant Chlorella Strain Screening and Its Damaging Effects on Photosynthesis. Frontiers in microbiology 9

Wasielesky Jr W, Atwood H, Stokes A, Browdy CL (2006) Effect of natural production in a zero exchange suspended microbial floc based super-intensive culture system for white shrimp *Litopenaeus vannamei*. Aquaculture 258:396-403

Zhang X, Ma L, Tian X, Huang H, Yang Q (2015a) Biodiversity study of intracellular bacteria closely associated with paralytic shellfish poisoning dinoflagellates *Alexandrium tamarense* and A. minutum. Int J Env Resour 4:23-27

Zhang X, Tian X, Ma L, Feng B, Liu Q, Yuan L, Fan C, Huang H, Yang Q (2015b) Biodiversity of the symbiotic bacteria associated with toxic marine Dinoflagellate *Alexandrium tamarens*e. Journal of Biosciences and Medicines 3:23

217 Zhuang Y, Zhang H, Hannick L, Lin S (2015) Metatranscriptome profiling reveals
218 versatile N-nutrient utilization, CO2 limitation, oxidative stress, and active toxin
219 production in an *Alexandrium fundyense* bloom. Harmful Algae 42:60-70
220

Journal of Applied Phycology: https://doi.org/10.1007/s10811-020-02049-9

Table 1. Summary of the experimental design assayed. The nitrogen concentrations correspond to those established in the culture medium at the beginning of each culture. All experiments were performed at an initial phosphate concentration of 181 μM in the culture medium. The N_T column represents the total nitrogen concentration provided from all the nitrogen sources.

Nº	Treatment	Nitrogen (N) source, μM			N_T, mg/L
		Nitrate-N	Urea-N	NH_4^+-N	
1	CTRL	882	0	0	12
2	AMO	0	0	882	12
3	URE	0	882	0	12
4	URE1	882	1000	0	26
5	URE2	882	2000	0	40
6	URE3	882	3500	0	61
7	URE4	882	5000	0	82
8	AMO1	882	0	1000	26
9	AMO2	882	0	2000	40
10	AMO3	882	0	3500	61
11	AMO4	882	0	5000	82
12	NUA1	441	441	1000	26
13	NUA2	882	1125	882	40
14	NUA3	1764	2150	441	61
15	NUA4	882	882	110	26

Journal of Applied Phycology: https://doi.org/10.1007/s10811-020-02049-9

Table 2. Progress of the acclimation of *Amphidinium carterae* to different sole nitrogen sources (nitrate, ammonium and urea) over three subcultivations (1, 2 and 3). Experiments CTRL, AMO and UREA are coded in Table 1. The kinetic parameters were measured in broth samples extracted at the end of every subculture. Data points are the averages along with their standard deviation for duplicate cultures. Values denoted by a different lowercase at each point for the same kinetic parameter, differ significantly at $p<0.05$ in the one-way ANOVA (degrees of freedom=5). Column *T* represents the direction of shift of each kinetic parameter in the acclimation process. V_c: Average cell volume; μ_{max}; maximum specific growth rate; C^c_{Bmax}: maximum cell concentration; C^b_{Bmax}: maximum biomass concentration expressed as dry weight; P^c_{Bmax}: maximum cell productivity; P^b_{Bmax}: maximum biomass productivity expressed as dry weight; F_V/F_M: maximum photochemical yield of photosystem II; *FL1,2,3*: cell fluorescence intensities measured by the photomultiplier detectors *FL1*, *FL2* and *FL3* in the flow cytometer; *SS* : cell side scatter.

Parameter	CTRL			
	1	2	3	T
V_C (×10^3), µm^3	1.39±0.23 ^{a}	1.30±0.05 ^{a}	1.52±0.17 ^{a}	↔
μ_{max}, day^{-1}	0.40±0.11 ^{a}	0.32±0.07 ^{a}	0.35±0.05 ^{a}	↔
C^c_{Bmax} (×10^5), cell·mL^{-1}	5.44±1.18 ^{a}	5.54±0.21 ^{a}	3.89±0.22 ^{a}	↔
P^c_{Bmax} (×10^4), cell·mL^{-1}·day^{-1}	5.88±1.23 ^{a}	5.40±0.32 ^{a}	3.55±0.22 ^{a}	↔
C^b_{Bmax}, g·L^{-1}	0.11±0.02 ^{a}	0.12±0.00 ^{a}	0.10±0.01 ^{a}	↔
P^b_{Bmax} (×10^{-2}), g·L^{-1}·d^{-1}	1.22±0.20 ^{a}	1.18±0.01 ^{a}	1.00±0.08 ^{a}	↔
Fv/Fm	0.55±0.04 ^{a}	0.50±0.04 ^{a}	0.50±0.09 ^{a}	↔
FL1 (x10^{-3}), a.u. µm^{-3}	14.37±0.61 ^{a}	15.09±0.81 ^{a}	18.10±1.24 ^{a}	↔
FL2 (x10^{-3}), a.u. µm^{-3}	9.26±0.07 ^{a}	10.85±0.05 ^{a}	15.72±2.88 ^{a}	↔
FL3 (x10^{-3}), a.u. µm^{-3}	9.62±0.21 ^{a,b}	8.35±0.38 ^{b}	11.11±0.87 ^{a}	↔
SS	4.18±0.09 ^{a}	4.21±0.10 ^{a}	4.46±0.18 ^{a}	↔
Parameter	AMO			
	1	2	3	T
V_C (×10^3), µm^3	1.60±0.68 ^{b}	2.14±0.45 ^{a,b}	3.08±0.05 ^{a}	↑
μ_{max}, day^{-1}	0.42±0.08 ^{b}	0.67±0.05 ^{b}	-0.29±0.01 ^{a}	↓
C^c_{Bmax} (×10^5), cell·mL^{-1}	4.42±0.33 ^{c}	2.07±0.35 ^{b}	0.04±0.00 ^{a}	↓
P^c_{Bmax} (×10^4), cell·mL^{-1}·day^{-1}	4.40±0.40 ^{c}	1.70±0.23 ^{b}	-0.15±0.01 ^{a}	↓
C^b_{Bmax}, g·L^{-1}	0.12±0.02 ^{c}	0.07±0.00 ^{b}	<0.01±0.00 ^{a}	↓
P^b_{Bmax} (×10^{-2}), g·L^{-1}·d^{-1}	1.31±0.21 ^{c}	0.74±0.05 ^{b}	-0.02±0.00 ^{a}	↓
Fv/Fm	0.54±0.04 ^{b}	0.47±0.08 ^{a,b}	0.18±0.04 ^{a}	↓
FL1 (x10^{-3}), a.u. µm^{-3}	8.45±1.54 ^{b}	13.55±2.51 ^{b}	118.93±0.61 ^{a}	↑
FL2 (x10^{-3}), a.u.µm^{-3}	5.15±1.19 ^{b}	5.80±0.74 ^{b}	86.97±1.30 ^{a}	↑
FL3 (x10^{-3}), a.u.µm^{-3}	3.88±0.39 ^{b}	8.01±1.05 ^{b}	34.66±2.75 ^{a}	↑
SS	4.39±0.13 ^{c}	5.78±0.07 ^{b}	14.19±0.29 ^{a}	↑
Parameter	URE			
	1	2	3	T
V_C (×10^3), µm^3	1.61±0.16 ^{b}	1.78±0.07 ^{b}	2.91±0.07 ^{a}	↑
μ_{max}, day^{-1}	0.52±0.16 ^{a}	0.49±0.09 ^{a}	0.38±0.07 ^{a}	↔
C^c_{Bmax} (×10^5), cell·mL^{-1}	4.15±0.29 ^{b}	2.17±0.23 ^{a}	1.20±0.15 ^{a}	↓
P^c_{Bmax} (×10^4), cell·mL^{-1}·day^{-1}	3.95±0.25 ^{b}	1.90±0.38 ^{a}	0.95±0.19 ^{a}	↓
C^b_{Bmax}, g·L^{-1}	0.12±0.01 ^{b}	0.07±0.01 ^{a}	0.06±0.01 ^{a}	↓
P^b_{Bmax} (×10^{-2}), g·L^{-1}·d^{-1}	1.29±0.12 ^{b}	0.63±0.15 ^{a}	0.62±0.08 ^{a}	↓
Fv/Fm	0.59±0.03 ^{b}	0.59±0.04 ^{b}	0.65±0.02 ^{a}	↑
FL1 (x10^{-3}), a.u. µm^{-3}	9.37±0.65 ^{b}	6.76±0.84 ^{a,b}	5.16±0.51 ^{a}	↓
FL2 (x10^{-3}), a.u. µm^{-3}	5.69±0.61 ^{b}	3.11±0.99 ^{a,b}	1.63±0.38 ^{a}	↓
FL3 (x10^{-3}), a.u. µm^{-3}	3.48±0.54 ^{b}	2.23±0.21 ^{a}	1.56±0.00 ^{a}	↓
SS	4.23±0.33 ^{a}	4.76±0.34 ^{a}	5.05±0.10 ^{a}	↔

Journal of Applied Phycology: https://doi.org/10.1007/s10811-020-02049-9

Table 3. Progress of the acclimation of *Amphidinium carterae* to different urea concentrations in presence of 882 µM nitrate through three subcultivations (1, 2 and 3). Experiments URE1 to URE4 are coded in Table 1. The kinetic parameters were measured in broth samples taken at the end of every subculture. Data points are averages along with their standard deviation for duplicate cultures. Values denoted by a different lowercase at each point, for the same kinetic parameter, differ significantly at $p<0.05$ in one-way ANOVA (degrees of freedom=5). The *T* column represents the direction of shift of every kinetic parameter in the acclimation process. V_c: Average cell volume; μ_{max}: maximum specific growth rate; C^c_{Bmax}: maximum cell concentration; C^b_{Bmax}: maximum biomass concentration expressed as dry weight; P^c_{Bmax}: maximum cell productivity; P^b_{Bmax}: maximum biomass productivity expressed as dry weight; F_V/F_M: maximum photochemical yield of photosystem II; *FL1,2,3*: cell fluorescence intensities measured by the photomultiplier detectors *FL1*, *FL2* and *FL3* of the flow cytometer; *SS*: side scatter of the cells.

Parameter	URE1				URE2			
	1	2	3	T	1	2	3	T
V_C (×10^3), µm^3	1.19±0.17 ^{a}	1.24±0.08 ^{a}	1.35±0.06 ^{a}	↔	1.24±0.26 ^{a}	1.22±0.09 ^{a}	1.46±0.15 ^{a}	↔
μ_{max}, day^{-1}	0.38±0.00 ^{a}	0.27±0.03 ^{a}	0.35±0.09 ^{a}	↔	0.39±0.10 ^{a}	0.30±0.05 ^{a}	0.39±0.03 ^{a}	↔
C^c_{Bmax} (×10^5), cell·mL^{-1}	6.05±0.52 ^{b}	5.11±0.22 ^{a,b}	3.75±0.20 ^{a}	↓	5.25±0.78 ^{b}	5.20±0.27 ^{b}	3.54±0.19 ^{a}	↓
P^c_{Bmax} (×10^4), cell·mL^{-1}·day^{-1}	6.23±0.41 ^{b}	4.95±0.31 ^{a,b}	3.53±0.21 ^{a}	↓	5.36±1.04 ^{b}	5.27±0.25 ^{b}	3.29±0.24 ^{a}	↓
C^b_{Bmax}, g·L^{-1}	0.12±0.01 ^{b}	0.11±0.01 ^{a,b}	0.09±0.00 ^{a}	↓	0.11±0.01 ^{b}	0.11±0.00 ^{b}	0.09±0.00 ^{a}	↓
P^b_{Bmax} (×10^{-2}), g·L^{-1}·d^{-1}	1.25±0.12 ^{b}	1.04±0.18 ^{a,b}	0.86±0.01 ^{a}	↓	1.16±0.05 ^{b}	1.11±0.02 ^{b}	0.88±0.06 ^{a}	↓
Fv/Fm	0.44±0.01 ^{a}	0.48±0.04 ^{a}	0.56±0.09 ^{a}	↔	0.52±0.06 ^{a}	0.48±0.04 ^{a}	0.56±0.02 ^{a}	↔
FL1 (x10^{-3}), a.u. µm^{-3}	11.87±0.65 ^{b}	16.87±1.51 ^{a}	18.12±0.33 ^{a}	↑	11.97±0.55 ^{b}	16.82±0.87 ^{a,b}	18.05±1.53 ^{a}	↑
FL2 (x10^{-3}), a.u. µm^{-3}	7.03±1.41 ^{b}	13.18±0.03 ^{a}	14.55±1.04 ^{a}	↑	6.37±0.65 ^{b}	11.35±0.40 ^{a,b}	14.91±3.00 ^{a}	↑
FL3 (x10^{-3}), a.u. µm^{-3}	8.31±0.11 ^{a}	6.41±0.76 ^{b}	8.51±0.58 ^{a}	↑	9.03±1.17 ^{a,b}	7.44±0.56 ^{b}	9.47±0.38 ^{a}	↑
SS	4.22±0.01 ^{a}	4.19±0.28 ^{a}	4.39±0.11 ^{a}	↔	4.90±0.20 ^{a}	4.87±0.09 ^{a}	4.89±0.21 ^{a}	↔
Parameter	URE3				URE4			
	1	2	3	T	1	2	3	T
V_C (×10^3), µm^3	1.13±0.43 ^{a}	1.20±0.02 ^{a}	1.51±0.26 ^{a}	↔	1.04±0.23 ^{b}	1.47±0.30 ^{a,b}	1.85±0.00 ^{a}	↑
μ_{max}, day^{-1}	0.45±0.02 ^{b}	0.28±0.02 ^{a}	0.39±0.06 ^{a,b}	↔	0.61±0.13 ^{a}	0.70±0.03 ^{a}	0.56±0.00 ^{a}	↔
C^c_{Bmax} (×10^5), cell·mL^{-1}	6.03±1.77 ^{a,b}	7.27±0.64 ^{b}	4.01±0.83 ^{a}	↓	3.43±0.63 ^{a,b}	4.86±0.00 ^{b}	2.35±0.05 ^{a}	↓
P^c_{Bmax} (×10^4), cell·mL^{-1}·day^{-1}	6.20±2.08 ^{b}	5.27±0.25 ^{b}	3.29±0.24 ^{a}	↓	3.39±0.93 ^{a,b}	5.15±0.06 ^{b}	2.16±0.00 ^{a}	↓
C^b_{Bmax}, g·L^{-1}	0.11±0.01 ^{a,b}	0.15±0.01 ^{b}	0.10±0.00 ^{a}	↓	0.06±0.01 ^{a}	0.11±0.03 ^{b}	0.07±0.00 ^{a}	↓
P^b_{Bmax} (×10^{-2}), g·L^{-1}·d^{-1}	1.16±0.10 ^{b}	1.11±0.02 ^{b}	0.88±0.06 ^{a}	↓	0.61±0.00 ^{a}	1.24±0.38 ^{b}	0.76±0.01 ^{a}	↓
Fv/Fm	0.51±0.03 ^{a}	0.48±0.07 ^{a}	0.56±0.09 ^{a}	↔	0.51±0.05 ^{a}	0.43±0.04 ^{b}	0.53±0.02 ^{a}	↑
FL1 (x10^{-3}), a.u. µm^{-3}	15.25±0.21 ^{a,b}	13.03±0.38 ^{b}	17.97±0.96 ^{a}	↑	19.14±2.26 ^{b}	12.63±1.84 ^{a}	17.18±0.24 ^{a,b}	↔
FL2 (x10^{-3}), a.u. µm^{-3}	7.63±2.02 ^{b}	7.32±0.92 ^{b}	13.70±0.80 ^{a}	↑	9.79±0.99 ^{a,b}	7.78±0.06 ^{b}	10.99±0.45 ^{a}	↑
FL3 (x10^{-3}), a.u. µm^{-3}	15.62±1.47 ^{a}	13.74±0.41 ^{a}	14.96±0.83 ^{a}	↔	13.04±1.71 ^{b}	6.61±0.72 ^{a}	8.65±0.46 ^{a}	↓
SS	4.98±0.08 ^{a}	4.61±0.17 ^{a}	5.01±0.31 ^{a}	↔	6.69±0.27 ^{a}	4.96±0.07 ^{b}	6.49±0.06 ^{a}	↑

Journal of Applied Phycology: https://doi.org/10.1007/s10811-020-02049-9

Table 4. Progress of the acclimation of *Amphidinium carterae* to different ammonium concentrations in the presence of 882 µM nitrate over three subcultivations (1, 2 and 3). Experiments AMO1 to AMO4 are coded in Table 1. The kinetic parameters were measured in broth samples taken at the end of every subculture. Data points are averages along with their standard deviation for duplicate cultures. Values denoted by a different lowercase at each point, for the same kinetic parameter, differ significantly at $p<0.05$ in the one-way ANOVA (degrees of freedom=5). The T column represents the direction of shift of every kinetic parameter in the acclimation process. V_c: Average cell volume; μ_{max}: maximum specific growth rate; C^c_{Bmax}: maximum cell concentration; C^b_{Bmax}: maximum biomass concentration expressed as dry weight; P^c_{Bmax}: maximum cell productivity; P^b_{Bmax}: maximum biomass productivity expressed as dry weight; F_V/F_M: maximum photochemical yield of photosystem II; *FL1,2,3*: cell fluorescence intensities measured by the photomultiplier detectors *FL1*, *FL2* and *FL3* of the flow cytometer; *SS*: side scatter of the cells. (The symbol -- means that there were no cells left at the end of the subculture)

Parameter	AMO1				AMO2			
	1	2	3	T	1	2	3	T
V_C (×10^3), µm^3	2.76±0.11 ^{a}	2.81±0.20 ^{a}	2.89±0.12 ^{a}	↔	--	--	--	--
μ_{max}, day^{-1}	-0.30±0.15 ^{a}	-0.35±0.08 ^{a}	-0.26±0.06 ^{a}	↔	-0.60±0.01 ^{a}	-0.60±0.00 ^{a}	-0.58±0.01 ^{a}	↔
C^c_{Bmax} (×10^5), cell·mL^{-1}	0.09±0.03 ^{a}	0.09±0.00 ^{a}	0.10±0.02 ^{a}	↔	--	--	--	--
P^c_{Bmax} (×10^4), cell·mL^{-1}·day^{-1}	-0.31±0.06 ^{b}	-0.51±0.03 ^{a}	-0.51±0.04 ^{a}	↓	-0.28±0.08 ^{a}	-0.46±0.00 ^{a}	-0.42±0.00 ^{a}	↔
C^b_{Bmax}, g·L^{-1}	<0.01±0.00 ^{a}	<0.01±0.00 ^{a}	<0.01±0.00 ^{a}	↔	--	--	--	--
P^b_{Bmax} (×10^{-2}), g·L^{-1}·d^{-1}	-0.03±0.02 ^{a}	-0.04±0.01 ^{a}	-0.04±0.02 ^{a}	↔	-0.05±0.01 ^{a}	-0.05±0.02 ^{a}	-0.07±0.00 ^{a}	↔
Fv/Fm	0.39±0.03 ^{a}	0.38±0.01 ^{a}	0.29±0.12 ^{a}	↔	--	--	--	--
FL1 (x10^{-3}), a.u. µm^{-3}	79.37±11.83 ^{a}	83.68±11.26 ^{a}	85.96±3.31 ^{a}	↔	--	--	--	--
FL2 (x10^{-3}), a.u. µm^{-3}	53.84±9.37 ^{a}	56.91±10.62 ^{a}	58.88±2.54 ^{a}	↔	--	--	--	--
FL3 (x10^{-3}), a.u. µm^{-3}	30.52±2.56 ^{a}	29.20±0.37 ^{b}	29.61±4.84 ^{a}	↔	--	--	--	--
SS	11.68±0.75 ^{a}	12.27±0.18 ^{a}	12.58±0.70 ^{a}	↔	--	--	--	--
Parameter	AMO3				AMO4			
	1	2	3	T	1	2	3	T
V_C (×10^3), µm^3	--	--	--	--	--	--	--	--
μ_{max}, day^{-1}	-0.68±0.11 ^{a}	-0.70±0.11 ^{a}	-0.66±0.10 ^{a}	↔	-0.60±0.14 ^{a}	-0.62±0.05 ^{a}	-0.59±0.14 ^{a}	↔
C^c_{Bmax} (×10^5), cell·mL^{-1}	--	--	--	--	--	--	--	--
P^c_{Bmax} (×10^4), cell·mL^{-1}·day^{-1}	-0.42±0.05 ^{b}	-0.46±0.00 ^{b}	-0.42±0.00 ^{a}	↔	-0.30±0.02 ^{a}	-0.39±0.06 ^{a}	-0.35±0.06 ^{a}	↔
C^b_{Bmax}, g·L^{-1}	--	--	--	--	--	--	--	--
P^b_{Bmax} (×10^{-2}), g·L^{-1}·d^{-1}	-0.07±0.01 ^{a}	-0.05±0.02 ^{a}	-0.07±0.02 ^{a}	↔	-0.06±0.01 ^{b}	-0.04±0.00 ^{a}	-0.03±0.01 ^{a}	↔
Fv/Fm	--	--	--	--	--	--	--	--
FL1 (x10^{-3}), a.u. µm^{-3}	--	--	--	--	--	--	--	--
FL2 (x10^{-3}), a.u.µm^{-3}	--	--	--	--	--	--	--	--
FL3 (x10^{-3}), a.u.µm^{-3}	--	--	--	--	--	--	--	--
SS	--	--	--	--	--	--	--	--

Journal of Applied Phycology: https://doi.org/10.1007/s10811-020-02049-9

Table 5. Nutrient removal efficiency (Γ, %) and P-molar formula of *A. carterae* biomass in those treatments where acclimation was attained in subcultivation 3. Data points are averages along with their standard deviation for duplicate cultures.

Treatment	$\Gamma_{NO_3^-}$ (%)	Γ_{urea} (%)	$\Gamma_{NH_4^+}$ (%)	Γ_{N_T} (%)	Γ_{P_T} (%)	*P-molar formula*
CTRL	53.2±2.1	--	--	53.2±2.1	62.2±2.4	$C_{39.3}\ O_{22.9}\ H_{72.8}\ N_{3.8}\ S_{0.2}\ P_1$
URE	--	49.6±3.4	--	49.6±3.4	74.2±1.8	$C_{40.5}\ O_{17.0}\ H_{70.1}\ N_{5.5}\ S_{0.2}\ P_1$
URE1	34.2±3.4	12.6±1.2	--	22.7±2.2	61.2±3.1	$C_{32.1}\ O_{17.7}\ H_{56.7}\ N_{3.4}\ S_{0.2}\ P_1$
URE2	37.4±7.4	7.4±3.5	--	16.6±4.7	60.0±3.6	$C_{32.6}\ O_{15.6}\ H_{58.3}\ N_{4.1}\ S_{0.2}\ P_1$
URE3	36.0±3.0	10.9±7.4	--	16.0±5.3	66.7±3.4	$C_{41.4}\ O_{22.5}\ H_{73.2}\ N_{6.8}\ S_{0.2}\ P_1$
URE4	26.0±5.0	14.6±2.5	--	16.3±1.3	68.7±3.4	$C_{30.2}\ O_{14.4}\ H_{59.4}\ N_{7.9}\ S_{0.2}\ P_1$
NUA4	50.8±2.9	16.9±4.4	87.0±1.4	37.0±3.3	63.4±4.4	$C_{44.6}\ O_{21.7}\ H_{78.8}\ N_{6.3}\ S_{0.2}\ P_1$

Journal of Applied Phycology: https://doi.org/10.1007/s10811-020-02049-9

Table 6. Progress of the acclimation of *Amphidinium carterae* using the three nitrogen sources (nitrate, ammonium and urea) together in the culture medium, over three subcultivations (1, 2 and 3). Experiments NUA1 to NUA4 are coded in Table 1. The kinetic parameters were measured in broth samples taken at the end of every subculture. Data points are averages along with their standard deviation for duplicate cultures. Values denoted by a different lowercase at each point, for the same kinetic parameter, differ significantly at $p<0.05$ in the one-way ANOVA (degrees of freedom=5). The T column represents the direction of shift of every kinetic parameter in the acclimation process. V_c: Average cell volume; μ_{max}: maximum specific growth rate; C^c_{Bmax}: maximum cell concentration; C^b_{Bmax}: maximum biomass concentration expressed as dry weight; P^c_{Bmax}: maximum cell productivity; P^b_{Bmax}: maximum biomass productivity expressed as dry weight; F_V/F_M: maximum photochemical yield of photosystem II; *FL1,2,3*: cell fluorescence intensities measured by the photomultiplier detectors *FL1*, *FL2* and *FL3* of the flow cytometer; *SS*: side scatter of the cells. (The symbol -- means that there were no cells left at the end of the subculture).

Parameter	NUA1				NUA2			
	1	2	3	T	1	2	3	T
V_C (×10³), µm³	2.22±0.16	2.83±0.40	--	--	1.92±0.10	2.66±0.15	--	--
μ_{max}, day⁻¹	0.39±0.04 ^{c}	0.07±0.01 ^{b}	-0.47±0.01 ^{a}	↓	0.38±0.02 ^{c}	0.09±0.02 ^{b}	-0.53±0.08 ^{a}	↓
C^c_{Bmax} (×10⁵), cell·mL⁻¹	0.97±0.06	0.70±0.06	--	--	1.55±0.14	0.84±0.04	--	--
P^c_{Bmax} (×10⁴), cell·mL⁻¹·day⁻¹	0.77±0.06 ^{c}	0.46±0.07 ^{b}	-0.45±0.02 ^{a}	↓	1.44±0.16 ^{c}	0.62±0.05 ^{b}	-0.41±0.02 ^{a}	↓
C^b_{Bmax}, g·L⁻¹	0.03±0.00	0.02±0.00	--	--	0.05±0.01	0.03±0.00	--	--
P^b_{Bmax} (×10⁻²), g·L⁻¹·d⁻¹	0.30±0.04 ^{c}	0.16±0.03 ^{b}	-0.09±0.02 ^{a}	↓	0.48±0.06 ^{c}	0.20±0.02 ^{b}	-0.10±0.01 ^{a}	↓
Fv/Fm	0.50±0.03	0.21±0.01	--	--	0.54±0.02	0.31±0.15	--	--
FL1 (x10⁻³), a.u. µm⁻³	72.44±6.45	86.93±7.74	--	--	47.43±2.23	54.62±5.91	--	--
FL2 (x10⁻³), a.u. µm⁻³	19.61±2.28	79.39±3.38	--	--	22.77±2.51	44.32±3.28	--	--
FL3 (x10⁻³), a.u. µm⁻³	30.61±2.99	33.85±3.54	--	--	5.03±1.35	7.95±3.16	--	--
SS	5.91±0.42	7.61±0.55	--	--	4.48±0.23	8.65±0.49	--	--
Parameter	NUA3				NUA4			
	1	2	3	T	1	2	3	T
V_C (×10³), µm³	1.52±0.25 ^{c}	2.14±0.08 ^{b}	3.02±0.35 ^{a}	↑	1.09±0.18 ^{a}	1.05±0.04 ^{a}	1.18±0.14 ^{a}	↔
μ_{max}, day⁻¹	0.37±0.02 ^{b}	0.13±0.04 ^{b}	-0.02±0.01 ^{a}	↓	0.43±0.07 ^{a}	0.39±0.01 ^{a}	0.41±0.01 ^{a}	↔
C^c_{Bmax} (×10⁵), cell·mL⁻¹	5.15±0.19 ^{c}	2.74±0.20 ^{b}	0.31±0.08 ^{a}	↓	6.79±1.47 ^{a}	6.70±0.25 ^{a}	4.96±0.28 ^{a}	↔
P^c_{Bmax} (×10⁴), cell·mL⁻¹·day⁻¹	5.46±0.21 ^{c}	2.69±0.23 ^{b}	-0.10±0.10 ^{a}	↓	7.16±1.67 ^{a}	7.05±0.29 ^{a}	5.07±0.32 ^{a}	↔
C^b_{Bmax}, g·L⁻¹	0.12±0.00 ^{c}	0.04±0.00 ^{b}	0.01±0.00 ^{a}	↓	0.11±0.02 ^{a}	0.14±0.02 ^{a}	0.11±0.01 ^{a}	↔
P^b_{Bmax} (×10⁻²), g·L⁻¹·d⁻¹	1.30±0.01 ^{c}	0.39±0.00 ^{b}	-0.01±0.00 ^{a}	↓	1.21±0.20 ^{a}	1.53±0.23 ^{a}	1.16±0.07 ^{a}	↔
Fv/Fm	0.57±0.02 ^{c}	0.43±0.01 ^{b}	0.30±0.02 ^{a}	↓	0.55±0.02 ^{a}	0.54±0.02 ^{a}	0.54±0.04 ^{a}	↔
FL1 (x10⁻³), a.u. µm⁻³	21,10±0.26 ^{b}	33.77±3.39 ^{b}	75.06±3.85 ^{a}	↑	17.97±0.76 ^{b}	19.62±1.05 ^{a,b}	24.43±1.68 ^{a}	↑
FL2 (x10⁻³), a.u.µm⁻³	13.60±0.51 ^{c}	30.51±3.67 ^{b}	64.62±4.17 ^{a}	↑	11.57±0.08 ^{a}	14.10±0.07 ^{a}	21.23±3.89 ^{a}	↔
FL3 (x10⁻³), a.u.µm⁻³	14.13±0.73 ^{c}	21.82±1.87 ^{b}	30.38±1.18 ^{a}	↑	12.02±0.26 ^{a,b}	10.86±0.50 ^{b}	15.00±1.18 ^{a}	↑
SS	4.59±0.04 ^{c}	7.57±0.31 ^{b}	10.62±0.70 ^{a}	↑	4.16±0.24 ^{a}	4.31±0.25 ^{a}	4.45±0.02 ^{a}	↔

Journal of Applied Phycology: https://doi.org/10.1007/s10811-020-02049-9

Table 7. Representative experiments from Table 1 (right column) in which the concentration levels of the main nutrients were higher than those reported for different aquaculture effluents**.** When available from literature, information on the microalgae used for each treatment of the effluents is included. The experiments of Table 1 placed in the right column are distributed in two groups in function of an effect deleterious or favourable on the growth according to the analysis carried out in Tables 2 to 4 and 6. SW: seawater, FW: freshwater:

Microalgae	Source	Water	Nutrients, $mg \cdot L^{-1}$				Representative experiments from Table 1	
			NO_3^--N	Urea-N	NH_4^+-N	PO_4^{3-}-P	Favorable	Deleterious
Skeletonema costatum.	(Hussenot et al. 1998)	SW	1.1	--	--	0.3	CTRL, URE1-4, NUA4	AMO1-4, NUA1-3
S. costatum.	(Hussenot et al. 1998)	SW	0.2	--	--	0.4	CTRL, URE1-4, NUA4	AMO1-4, NUA1-3
Platymonas sub cordiformis.	(Guo et al. 2013)	SW	1.7	--	0.5	0.2	NUA4	AMO1-4, NUA1-3
Chlorella sp.	(Nasir et al. 2015)	FW	--	--	--	2.6	CTRL, URE, URE1-4, NUA4,	AMO, AMO1-4, NUA1-3
Chlorella vulgaris. Scenedesmus obliquus. Chaetoceros calcitrans	(Gao et al. 2016)	SW	2.0	--	--	--	CTRL, URE1-4, NUA4,	AMO1-4, NUA1-3
Oocystis borgey	(Liu et al. 2018)	SW	0.8	1.0	0.8	--	NUA4	NUA1-3
Tetraselmis suecica.	(Andreotti et al. 2017)	SW	4.0	--	0.3	0.3	NUA4	AMO1-4, NUA1-3
Dunaliella tertiolecta.	(Andreotti et al. 2017)	SW	4.1	--	0.3	0.6	NUA4	AMO1-4, NUA1-3
Isochrysis galbana	(Andreotti et al. 2017)	SW	4.2	--	0.3	0.6	NUA4	AMO1-4, NUA1-3
Oocystis sp.	(Riaño et al. 2011)	FW	--	--	13.7	--	--	AMO1-4, NUA1
Oocystis sp.	(Riaño et al. 2011)	FW	--	--	17.3	--	--	AMO2-4
Tetraselmis chuii.	(Khatoon et al. 2018)	SW	--	--	5.3	5.6	--	AMO, AMO1-4, NUA1-3
Tetraselmis sp. Stauroneis sp. Phaeodactylum sp.	(Li et al. 2019)	SW	5.1	--	0.4	0.3	NUA4	AMO1-4, NUA1-3
Tetraselmis suecica	(Andreotti et al. 2019)	SW	3.8	--	0.1	0.7	NUA4	AMO1-4, NUA1-3
Dunaliella tertiolecta	(Andreotti et al. 2019)	SW	2.9	--	0.4	0.6	NUA4	AMO1-4, NUA1-3
Phaeodactylum tricornutum	(Borges et al. 2005)	SW	0.6	--	4.9	0.7	--	AMO1-4, NUA1-3
Isochrysis galbana.	(Borges et al. 2005)	SW	0.9	--	0.4	0.6	NUA4	AMO1-4, NUA1-3
Tetraselmis suecica.	(Borges et al. 2005)	SW	0.2	--	1.4	0.3	NUA4	AMO1-4, NUA1-3
Synechococcus sp.	(Srimongkol et al. 2019)	SW	--	--	16.5	0.4	--	AMO2-4
Chlorella sorokiniana.	(Chen et al. 2019)	FW	12.3	--	8.1	0.4	--	AMO1-4, NUA2
Chlorella sp. Scenedesmus quadricuada	(Halfhide et al. 2014)	SW	18.1	--	--	2.1	--	NUA3
--	(Halfhide et al. 2014; Hussenot et al. 1998)	SW	0.2	0.6	0.6	0.2	NUA4	NUA1-3
--	(Pagand et al. 2000)	SW	8.2	--	--	1.3	CTRL, URE1-4, NUA4,	AMO1-4, NUA2-3
--	(Deviller et al. 2004)	SW	14.5	--	0.3	1.7	--	NUA3
--	(Schulz et al. 2003)	FW	0.7	--	0.6	0.4	NUA4	AMO1-4, NUA1-3

Journal of Applied Phycology: https://doi.org/10.1007/s10811-020-02049-9

Legends

Fig. 1. Variation in C_B^c/C_{Bo}^c versus culture time for the third subculture of each treatment, the kinetic parameters of each are displayed in Tables 2 to 4. Experiments are encoded in Table 1. Solid and dashed lines show Eq. (1) predictions. Experimental data are given as the average of the duplicate cultures ±SD. The nitrogen sources are: A) a sole N-source (nitrate, ammonium or urea); B) nitrate and ammonia; and C) nitrate and urea; D) nitrate, ammonium and urea.

Fig. 2. Microbial species biodiversity analysis of the symbiotic bacteria of *Amphidinium carterae* grown in a long-term raceway open pond using nitrate as the sole nitrogen source, as earlier described (Molina-Miras et al. 2018a). The most predominant taxonomic categories were included.

Journal of Applied Phycology: https://doi.org/10.1007/s10811-020-02049-9

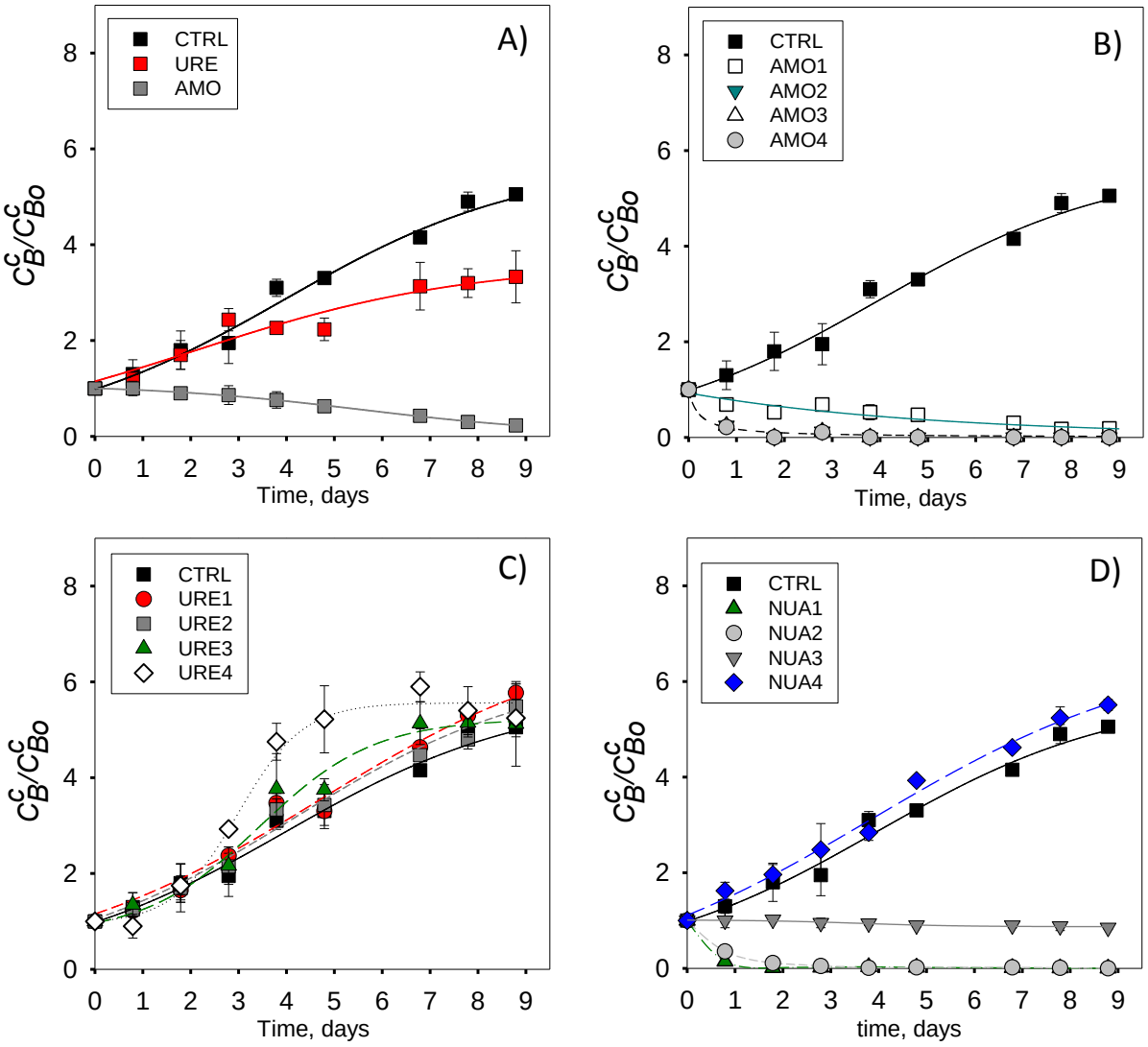

Figure 1

Journal of Applied Phycology: https://doi.org/10.1007/s10811-020-02049-9

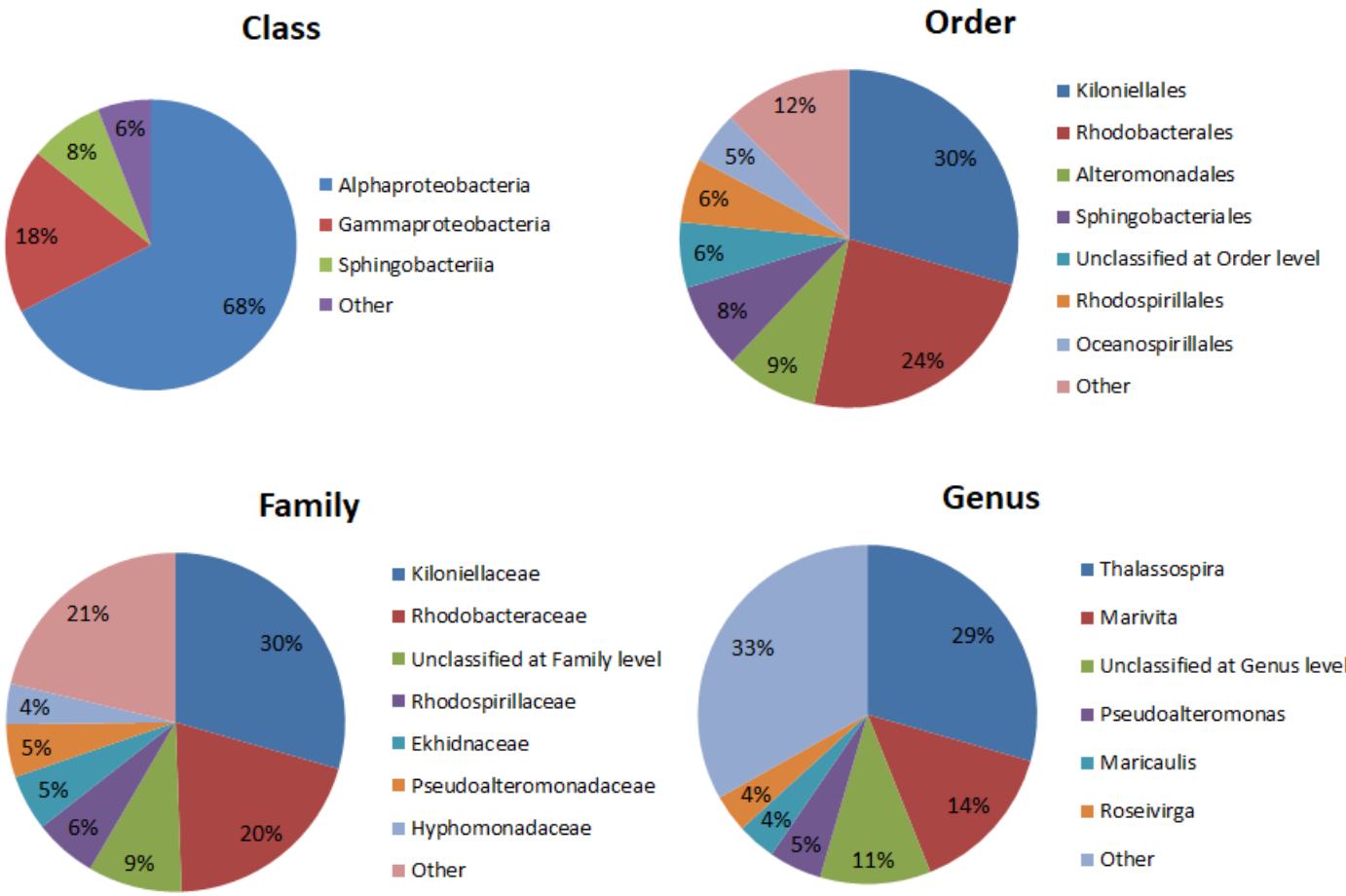

Figure 2